U-Pb zircon dating of the plutonic Hisingen suite in SW Sweden: geochemical classification and evaluation of field methods for differentiation

Max Nordqvist

Degree of Bachelor of Science
with a major in Earth Sciences
15 hec

Department of Earth Sciences
University of Gothenburg
2023 B-1181

Faculty of Science

UNIVERSITY OF GOTHENBURG

UNIVERSITY OF GOTHENBURG
Department of Earth Sciences
Geovetarcentrum/Earth Science Centre

U-Pb zircon dating of the plutonic Hisingen suite in SW Sweden: geochemical classification and evaluation of field methods for differentiation

Max Nordqvist

ISSN 1400-3821

B1181
Bachelor of Science thesis
Göteborg 2023

Mailing address
Geovetarcentrum
S 405 30 Göteborg

Address
Geovetarcentrum
Guldhedsgatan 5A

Telephone
031-786 19 56

Geovetarcentrum
Göteborg University
S-405 30 Göteborg
SWEDEN

Abstract

The aim of this study was to investigate the c. 1.5 Ga Hisingen suite and the c. 1.3 Ga Kungsbacka bimodal suite by LA–ICP–MS U–Pb zircon dating, geochemical classification, magnetic susceptibility, gamma ray spectrometry and handheld X–ray fluorescence analyses. Four rock samples were collected across a previously mapped contact between the two suites, and mineral separation was performed to isolate zircons for analysis. Zircon dating of two of the samples gave ages of 1556±8 Ma and 1557±6 Ma for this thesis, while the two others were dated by Winblad (2022), which gave ages between 1548–1538 Ma. These ages ascribe the rocks to the main part of the Hisingen suite continental arc magmatism at 1588–1522 Ma. None of the analyses showed ages coeval with the intraorogenic period when the Kungsbacka bimodal suite intruded. Previously collected and analyzed rocks were used to compare with and classify the newly collected rocks. The newly collected rocks were classified as magnesian, calc-alkalic granites and granodiorites, which are described by the literature as common in the plutonic parts of magmatic arcs. Trace element analysis revealed a possibly diagnostic signature of the Heavy Rare Earth Elements (HREE) between the Hisingen and some of the Kungsbacka suite rocks. No other diagnostic trends were identified by magnetic susceptibility, gamma ray radiation or XRF analysis. A comparison between handheld XRF analysis and whole-rock chemical analysis showed that the XRF performs well for certain elements that can be useful when characterizing granitic rocks.

Keywords: U–Pb dating, zircon, total whole rock chemistry, handheld XRF, magnetic susceptibility, gamma ray spectrometry, LA–ICP–MS, SEM, granite, granodiorite, Idefjorden Terrane, Sveconorwegian Province

Sammanfattning

Syftet med den här studien var att undersöka den c. 1.5 Ga Hisingensviten och den c. 1.3 Ga bimodala Kungsbackasviten genom LA–ICP–MS U–Pb zirkondatering, geokemisk klassificering, magnetisk susceptibilitet, mätning av gammastrålning samt analys genom handhållen röntgenstrålningsfluorescens (XRF). Fyra bergprov inhämtades över en tidigare karterad kontakt mellan de två sviterna och mineralseparation genomfördes för att isolera zirkoner för analys. Zirkondatering av två av proverna gav åldrar på 1556±8 Ma och 1557±6 Ma för den här uppsatsen, medan de två andra proverna daterades av Winblad (2022), och gav åldrar mellan 1548–1538 Ma. Dessa åldrar placerar de analyserade hällarna inom huvuddelen av Hisingensvitens konvergenta kontinentala magmatism vid 1588–1522 Ma. Inga analyser visade åldrar samtida med den intraorogena period då den bimodala Kungsbackasviten intruderade. Tidigare inhämtade och geokemiskt analyserade prover från båda sviterna användes för att jämföra med och klassificera de inhämtade proverna. De inhämtade proverna klassificerades som ’magnesiska’, kalk-alkalina graniter och granodioriter, vilka beskrivs i litteraturen som vanligt förekommande i de intrusiva delarna av magmatiska öbågar. Spårämnesanalys visade ett möjligt diagnostiskt mönster i halterna av de tunga sällsynta jordartsmetallerna (Heavy Rare Earth Elements, HREE) mellan Hisingensviten och delar av Kungsbackasviten. Inga andra diagnostiska trender identifierades via undersökningar av magnetisk susceptibilitet, gammastrålning eller XRF. En jämförelse mellan analys via handhållen XRF och ’totalt-berg’ kemisk analys visade att XRF–analys presterar bra för vissa ämnen som kan vara användbara vid karaktärisering av granitiska bergarter.

Nyckelord: *U–Pb datering, zirkon, handhållen XRF, magnetisk susceptibilitet, gammastrålning, aktivitetsindex, LA–ICP–MS, SEM, granit, granodiorit, Idefjorden terrängen, Svekonorvegiska provinsen*

Table of contents

Introduction

Background and aim

The main aim of this study is to evaluate field methods for differentiating two plutonic rock suites of different ages in the Gothenburg area of Sweden: the 1.5 Ga Hisingen suite, and the 1.3 Ga Kungsbacka bimodal suite. Traditionally, these rocks have been divided into different series based on their degree of deformation and metamorphic overprint, with higher degrees being interpreted as older emplacement ages (Samuelsson, 1985). More recent reviews and articles show a more varied picture and note the heterogeneity in composition and degrees of deformation of the bedrock in the Gothenburg area (Åhäll & Connelly, 2008; Petersson et al., 2015; Bergström et al., 2022). The similarities across the suites and heterogeneity within them, presents a difficulty when ascribing an emplacement age to the rocks in the field. Therefore, it would be of benefit to develop field methods that allows determination of what rock suite an outcrop belongs to.

Rock samples will be collected across a N–S striking contact between the Hisingen and Kungsbacka suites, mapped by the Swedish Geological Survey. Zircon U–Pb dating will be performed to determine the emplacement ages of the outcrops, since the mapped contacts may not be correct, due to this area being difficult to map. Coupled with the zircon dating, whole-rock geochemical and handheld X-ray fluorescence analyses as well as gamma ray spectrometry and magnetic susceptibility surveying will all be performed to examine if certain element-trends or diagnostic signatures can be used for differentiation of the suites.

The two main aims of this study are therefore:

- Determine emplacement ages of outcrops by zircon U–Pb dating across the mapped Hisingen and Kungsbacka suites contact.
- Evaluate the suitability of gamma ray spectrometry, magnetic susceptibility surveying and handheld XRF analysis for differentiation of the Hisingen and Kungsbacka rock suites by examining if diagnostic element- or data-signatures can be identified and applied in the field.

Geological background

The crystalline basement rocks of the Gothenburg area in Sweden are part of the Sveconorwegian province, located on the southwestern margin of the Fennoscandian shield (Fig. 1). The Sveconorwegian province accreted onto the Fennoscandian foreland in several stages during the Mesoproterozoic. The province is divided into five main lithotectonic units

which are separated by shear zones. The Eastern segment is parautochthonous with the Fennoscandian foreland to the east, while the rest of the units have experienced considerable transport during the orogeny and are therefore referred to as terranes; Telemarkia, Bamble, Kongsberg and Idefjorden. The Mylonite shear zone separates the Idefjorden terrane from the Eastern segment (Bingen et al., 2008).

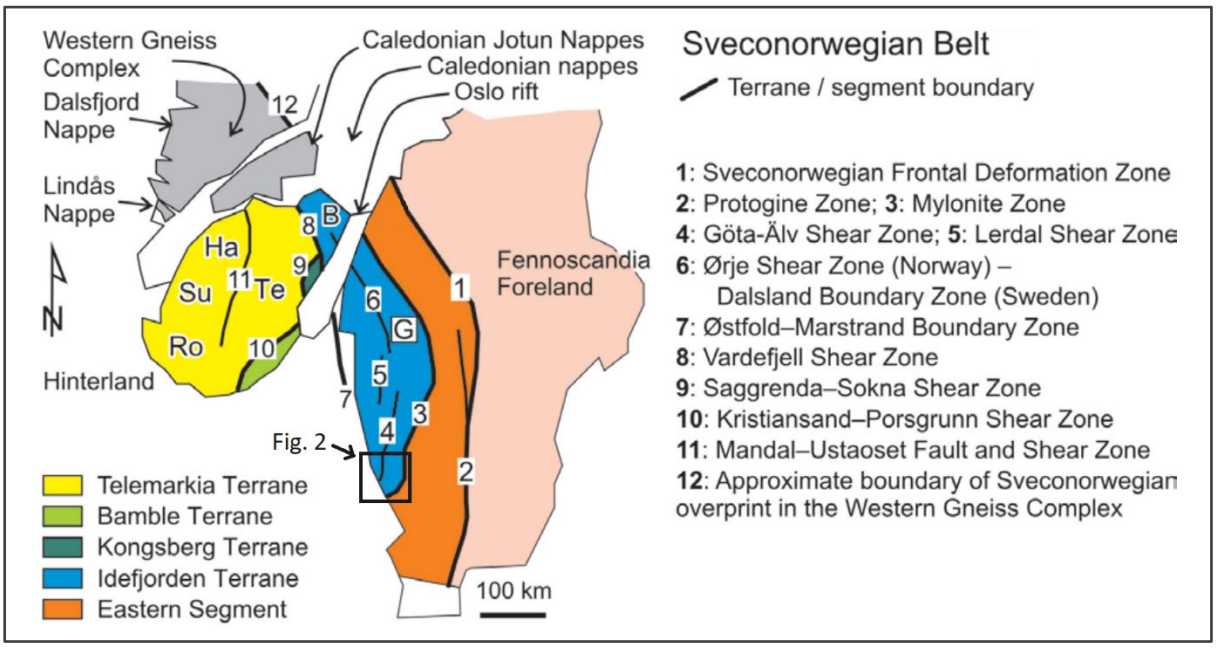

Figure 1. Regional geological map of southwestern Scandinavia showing lithotectonic units and shear zones of the Sveconorwegian province. Modified from Bingen et al. (2008).

The rocks that make up the Sveconorwegian province vary in age from c. 1.66–0.9 Ga and were formed during or metamorphosed by three developmental phases: two major orogenic events with an intraorogenic period in-between. The first orogeny is the Gothian orogeny at c. 1.66–1.5 Ga, during which calc-alkaline and tholeiitic plutonic and volcanic rocks were emplaced, and supracrustals were subjected to amphibolite facies metamorphism at c. 1.54 Ga (Bingen et al., 2008). The Gothian plutonic rocks have been divided into two separate suites, the older Gothenburg suite to the east and the younger Hisingen suite to the west. These suites are dominated by red and grey granitoids, but gabbros, diorites and tonalites also occur. Augen (porphyritic) varieties occur among the granitoids and have in some places been altered to augen gneisses (Lindström et al., 2011).

The second period of development in the Sveconorwegian province occurred between c. 1.5–1.15 Ga and is referred to as an intracratonic or intraorogenic period of high magmatic activity between the Gothian and Sveconorwegian orogeneses. During this period, rocks that intruded

the previously formed bedrock include the c. 1336–1311 Ma Askim granite and mafic Chalmers intrusion, which belong to the Kungsbacka bimodal suite, as well as older intrusive rocks to the north in Bohuslän like gabbro, dolerite and augen granite at c. 1500 Ma (Lindström et al., 2011).

The third period of development is the Sveconorwegian orogeny itself, which occurred between c. 1.15–0.9 Ga and is part of the larger Grenvillian orogeny, which is linked to the growth of the supercontinent Rodinia. Only limited formation of new bedrock occurred in the Swedish part of the Idefjorden terrane during the orogeny. Among the newly formed bedrock is the marine sedimentary Dal Formation, and intrusive rocks such as the Bohus granite, and the mafic Tuve dyke and associated dolerites (Hellström, 2009). The intrusive rocks were formed during the late or post-Sveconorwegian orogeny since they appear relatively undeformed and in cross-cutting relationships with Sveconorwegian deformational features. Rocks formed previously during the Gothian or intracratonic periods in the Idefjorden terrane were in large parts structurally and metamorphically overprinted during the Sveconorwegian orogeny. The metamorphic grade varies from greenschist- to amphibolite-facies, but locally up to granulite-facies conditions. Metamorphic and structural overprinting, and a lack of complete surveying of the older Gothian bedrock can make it hard to distinguish the effects of the Sveconorwegian orogeny from previous events (Lindström et al., 2011).

In older reports by SGU, the intrusive complexes in southwestern Sweden have been grouped into different series (A-D) based on their deformational and metamorphic history. The degree to which the rocks have been subjected to deformation and metamorphism have been interpreted to reflect their relative emplacement ages, with the A-series being the most deformed and therefore oldest (Samuelsson, 1985).

The A–D series terminology of the rocks in the Gothenburg area is still in use by geologists, even if the older estimations of emplacement ages of the complexes in some cases do not match what has been found by dating in more recent works. For example, Samuelsson (1985) ascribes an older augen granite (RA granite) to the B-series at c. 1650 Ma, and a younger augen granite (Askim granite) to the C-series at c. 1400 Ma. In recent articles they have both given ages of c. 1336–1311 Ma and are ascribed to the Kungsbacka bimodal suite (Hegardt et al., 2007).

Figure 2 shows a geological map of the Gothenburg area, with both the A–D series terminology and the more up to date ‘suite’ terminology being used. By geologists today, the Hisingen and Gothenburg suites are said to belong to the B-series intrusive complex, while the Kungsbacka bimodal suite is said to be part of the C-series of rocks. In recent summaries of the bedrock in

the Gothenburg area by SGU, the A-D series terminology is not used, and instead the name of suites and known emplacement ages are used (Bergström et al., 2022).

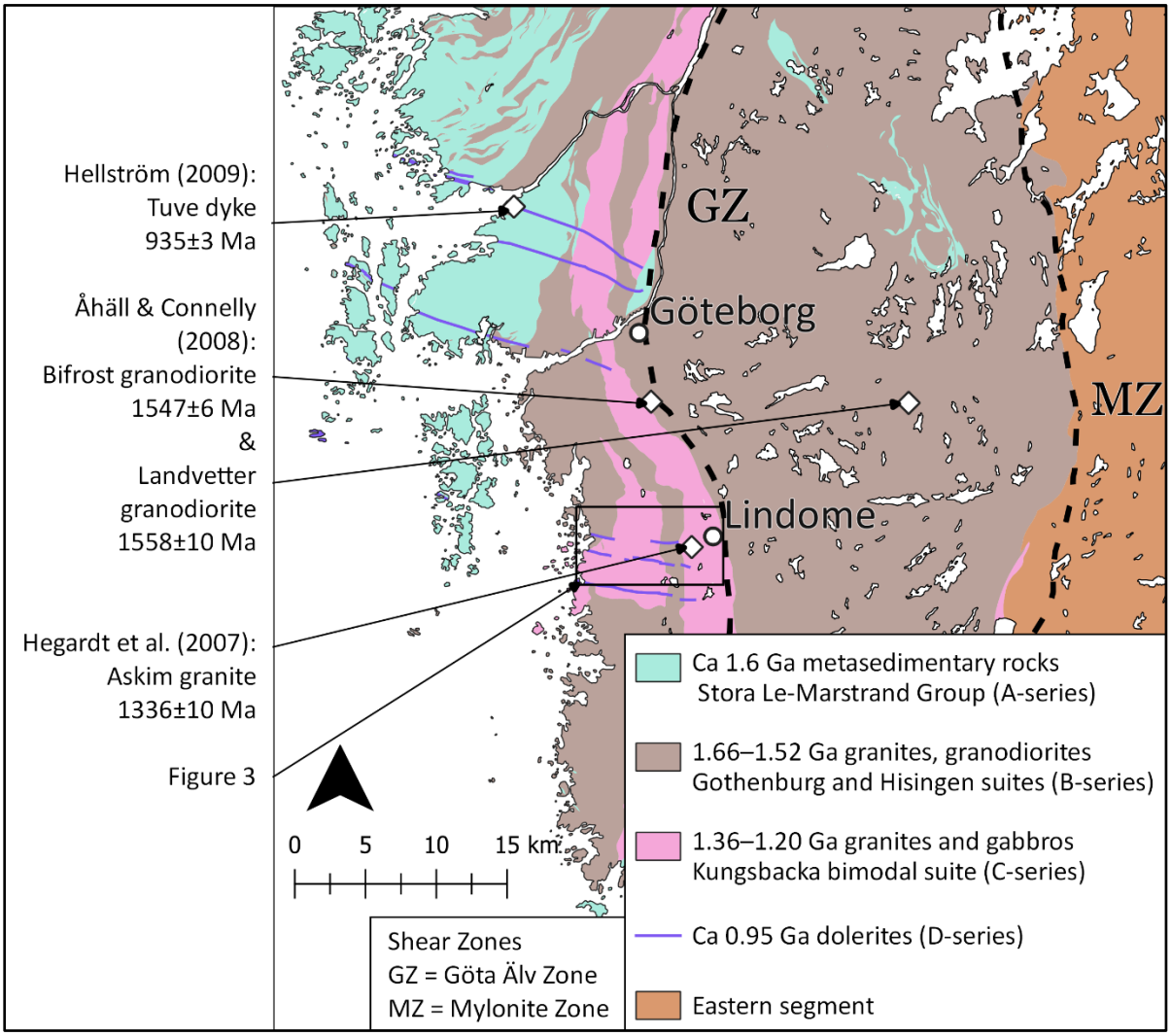

Figure 2. Geological overview map of the rocks of the Gothenburg area. Source data: SGU Bedrock map and Lantmäteriet GSD-Översiktskartan.

Hisingen suite

The Hisingen suite intruded the previously formed bedrock at c. 1588–1522 Ma during the Gothian orogeny. Examples of rocks in the Gothenburg area include the 1558±10 Ma Landvetter granodiorite and the 1547±6 Ma Bifrost granodiorite. Zircons from the Landvetter granodiorite also gave a statistically valid age of 1610±10 Ma, interpreted to be inherited from older Gothenburg suite rocks (Åhäll & Connelly, 2008). In the area around Askim and Frölunda, there is an alkali feldspar porphyritic granite of the Hisingen suite which is called the Frölunda granite. The composition of the suite varies, with three main types: dark grey equigranular tonalites to granodiorites, through lighter grey to reddish grey equigranular and porphyritic granodiorites and granites, and to red equigranular granites. These types are not

rigid, and overlapping can occur. Through magma mixing and mingling processes, coeval <1 m mafic enclaves occur in areas of the suite, and more intermediate hybrid rocks can be identified. Mineralogically the granodiorites and granites show quartz, plagioclase, and alkali feldspar in approximately equal amounts, plus biotite, while the more tonalitic rocks have more plagioclase and commonly hornblende. The rocks are only weakly gneissic, and very rarely banded, and thus primary magmatic textures are commonly preserved (Bergström et al., 2022).

Kungsbacka Bimodal suite

During the intracratonic period of development in the Sveconorwegian province, there were periods of bimodal magmatism where both felsic and mafic magmas intruded. Hybrid rocks occur due to magma-mixing like in the older Hisingen suite, but the mafic elements are much more prominent in the Kungsbacka suite. The mafic rocks of the suite consist of rocks of diorite to gabbro composition, while the felsic rocks are of granitic to granodioritic composition. The felsic rocks of the suite are mainly of two types: red-grey porphyritic granites to granodiorites, and red equigranular granites (Lundqvist & Kero, 2006). In the Gothenburg area, rocks in this suite include the Göta, Kärra, and Askim granites, and the mafic Chalmers intrusion, with ages between c. 1333–1304 Ma (Hegardt et al., 2007; Kiel et al., 2009). Characteristic of the granites of the suite is higher levels of gamma ray radiation. The highest amounts are found in the Kärra granite, which is also referred to as the RA granite (radioactive), due to high uranium and thorium contents. The U and Th contents of the RA granite can vary from 10–15 ppm U and 40–50 ppm Th (Lindström et al., 2011), compared to c. 1–2 ppm U and 5–10 ppm Th for rocks belonging to the Hisingen suite. The Askim granite also shows higher amounts of K, U and Th, compared to rocks belonging to other suites in the area (Bergström et al., 2022).

Study area

The area of interest for this study is situated between the communities Billdal and Lindome in southwestern Sweden, 15 km south of Gothenburg, along the road Spårhagavägen (Fig. 3). According to the SGU bedrock map, there is a c. 1–2 km wide and N-S striking unit of granites and granodiorites of the Hisingen suite in contact with Askim granites of the Kungsbacka bimodal suite on both sides. It is important to note that the contacts according to the bedrock map are approximate, and mapping of them by SGU has been done mainly according to visual properties like color, mineral content, deformation, and presence of feldspar phenocrysts (Erik Sturkell, personal communication).

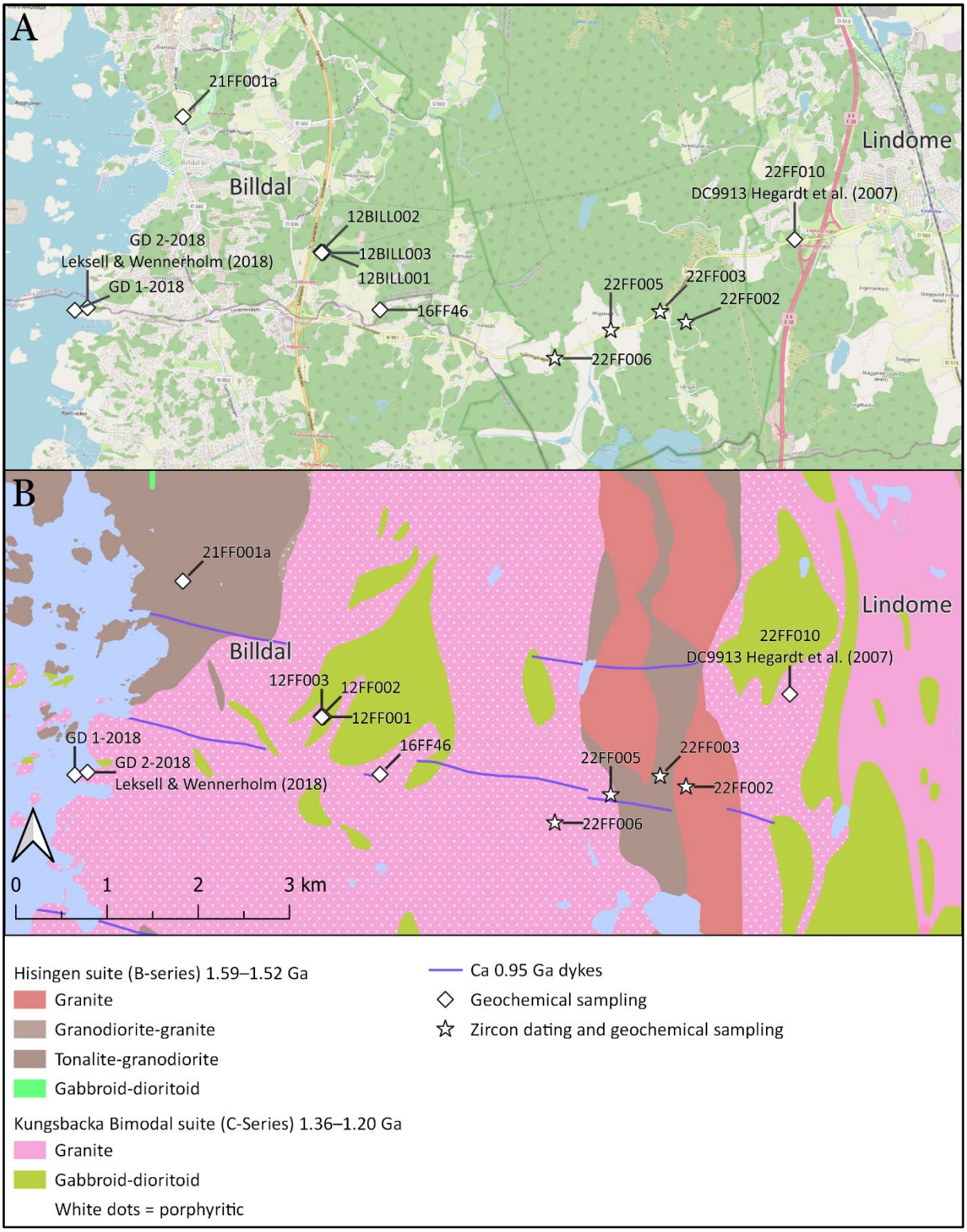

Figure 3. Overview of the study area with geochemical sampling points. (A) OpenStreetMap. (B) SGU bedrock map.

The Askim granite is described by SGU as a greyish red to reddish grey porphyritic granite. The feldspar phenocrysts are commonly 1–2 cm of rounded to rectangular shape, and sometimes of Rapakivi-type where the alkali feldspar is surrounded by a rim of plagioclase.

Locally there are enclaves of metamorphic diorite and gabbro of centimeter to meter size. During the Sveconorwegian orogeny between c. 1.15–0.9 Ga the granite was deformed in N-S striking patches as well as subjected to amphibolite facies metamorphism which means the rock can be strongly gneissic in some areas (Lundqvist & Kero, 2006). The Askim granite was dated from a sample collected at the type locality near Lindome by Hegardt et al. (2007) using the U–Pb zircon ion-microprobe method, which gave a result of 1336±10 Ma (Fig. 3).

The Hisingen suite rocks of the study area have been mapped as granodiorites and granites by SGU in their bedrock map. These rocks are quite similar to the Askim granite, but there can be some notable differences. As described by Lundqvist and Kero (2006), the composition of the Hisingen suite rocks vary from granitic to tonalitic, and the color from greyish red to dark grey, compared to the Askim granite which is more felsic and often more red in appearance. Features of note of the Hisingen suite rocks is that they most often are equigranular with a medium grain size, often contains small amounts of muscovite, and that the plagioclase grains contain small crystals of epidote, which give the plagioclase a greenish tint (Bergström et al., 2022). However, the greenish tint of the plagioclase can also be observed in rocks of the Kungsbacka suite, so it is not to be considered diagnostic.

As evident by the descriptions of the two rock types present at the study area according to the SGU bedrock map, they can be very similar, and determining what suite an outcrop belongs to in the field can be difficult. When comparing chemical and mineralogical data of the rocks in the Hisingen suite to the felsic rocks of the Kungsbacka bimodal suite, the Hisingen suite rocks are generally less felsic in composition, containing more iron and calcium, but lower amounts of potassium, uranium, and thorium (Lundqvist & Kero, 2006). The Kungsbacka suite felsic rocks are more grouped into the granite field of a Quartz-Alkali-Plagioclase (QAP or Streckeisen diagram) plot, while the Hisingen suite rocks vary in composition from granite to tonalite (Bergström et al., 2022).

Figure 4 shows a picture of the outcrop where sample 22FF002 was collected. The outcrop is located in an area mapped as a granite belonging to the Hisingen suite in the SGU bedrock map. In the field the rock is equigranular with low amounts of alkali feldspar at around 5%, the plagioclase often has a greenish tint and make up around 20–30% of the rock, and the quartz content is around 10–30%. The amount of darker minerals is high, with biotite constituting the majority, but hornblende can also be identified. Mafic enclaves 30–40 cm in size occur in areas of the rock. There is a slight foliation that dips to the west and several pegmatitic veins cut the rock.

Figure 4. Picture of an example of the rock outcrop where sample 22FF002 was collected. It was mapped by SGU as a granite belonging to the Hisingen suite. Note the low amounts of alkali feldspar, and mafic enclaves to the left in the picture. The diameter of the borehole is 5 cm.

Sample 22FF005 was collected at an outcrop mapped by SGU as a porphyritic Askim granite, very close to the contact with the Hisingen suite. A picture from the outcrop is shown in Figure 5. At the outcrop the rock has an overall red appearance due to the high amount of alkali feldspar, which is sometimes occurring as 1–2 cm phenocrysts. However, the rock is not observed to have the typical augen granite appearance associated with the Askim granite. The plagioclase can be estimated to around 5–10% and sometimes show a greenish tint, and the quartz content is around 20%. Biotite is common and shows a foliation with a linear and planar fabric that dips to the west.

Figure 5. Picture of the outcrop where sample 22FF005 was collected.

Gamma ray radiation and magnetic susceptibility of rocks

According to Bergström et al. (2022), another distinguishing factor of the two suites, beyond the silica content, can be the total amount of gamma ray radiation of the rocks. Gamma ray radiation can be expressed as activity index (AI), calculated from the activity concentrations of the three components ^{40}K, ^{226}Ra (^{238}U) and ^{232}Th. The activity index is calculated by the formula:

$$C_K/3000+C_{Ra}/300+C_{Th}/200$$

where C_K = activity of potassium in Bq/kg and 1% K = 313 Bq/kg ^{40}K, C_{Ra} = activity of radium in Bq/kg and 1 ppm U = 12.35 Bq/kg ^{226}Ra, and C_{Th} = activity of thorium in Bq/kg and 1 ppm Th = 4.06 Bq/kg ^{232}Th. Generally, more felsic rocks have higher amounts of the elements K, U and Th. Since the felsic rocks of the Kungsbacka bimodal suite generally are more felsic than the Hisingen suite according to Bergström et al. (2022), they show higher levels of gamma ray radiation due to these components (Table 1). The granodioritic–granitic rocks of the Hisingen suite have an activity index of around 0.7, while the more tonalitic rocks have a lower at around 0.3–0.4. The Askim granite has a higher activity index at around 1.0, while the RA granite is even higher at 1.7 or above. Local enrichment processes not yet well understood can also affect the rocks, which can produce especially high levels of

radioactive elements. However, one should be careful when comparing rocks by activity index since any anomalies in only one of the elements will be reduced when the index is calculated.

The magnetic susceptibility of a rock is the measurement of how much the rock becomes magnetized when a magnetic field is applied and is controlled by the presence of the mineral magnetite, but it can also be affected by structural and metamorphic overprinting. Magnetic susceptibility data from Bergström et al. (2022) is presented in Table 1. In the SI-system, the unit for magnetic susceptibility is dimensionless.

Table 1. Radiometric components including activity index, and magnetic susceptibility data from Bergström et al. (2022), of rocks possibly present at the study area. N shows the number of samples.

Rock type	K (%)	U (ppm)	Th (ppm)	Activity index	Susceptibility 10^{-3}	N
Hisingen suite B-series						
Granite	4.8	1.5	8.6	0.73		1
Granodiorite-granite	2.34	2.5	9.1	0.53	0.775	2
Granodiorite-gr, porphyritic	3.8	1.1	8.5	0.62		2
Tonalite-granodiorite	2	1.9	6.6	0.42	5.286	8
Kungsbacka suite C-series						
RA granite	4.34	12.3	40.9	1.79	1.519	7
Askim granite	4.55	4.6	25.1	1.17	6.511	6
Askim granodiorite	2.73	2.53	9.48	0.58	0.705	4

U–Pb zircon geochronology

Using long-lived radioactive decay systems like $^{238}U \rightarrow {}^{206}Pb$ and $^{235}U \rightarrow {}^{207}Pb$ provides us with the best possibility to construct a coherent geological history of the Earth. During crystallization, zircon incorporates U and Th in its crystal structure (generally 10–1000 ppm U and 1–100 ppm Th), while it strongly excludes Pb. The Pb/U ratio of zircon at formation is therefore very low. The long-lived radioactive isotopes ^{238}U and ^{235}U of uranium decay to stable isotopes of lead (^{206}Pb and ^{207}Pb, respectively), ^{232}Th decays to stable ^{208}Pb, while the stable ^{204}Pb has no parent isotope. Lead that is not formed by radioactive decay, also known as common lead, is rare in zircon. The Pb/U ratio of the zircon grains will increase as the grain

age and radioactive decay occurs. Since the half-lives of the parent isotopes of lead are known, finding the ratio of parent/daughter isotopes in a zircon grain allows the determination of when the system was closed, and no new parent isotopes were added. However, loss of lead can occur due to various events, like metamorphism or diffusion, which will disturb the final ratios of parent/daughter isotopes. Despite this, zircon is the most widely used mineral for geochronology, due to its ability to incorporate U, and being able to preserve its U and Pb contents through metamorphic events (Davis et al., 2003; Parrish & Noble, 2003).

Determination of the ratios of parent/daughter isotopes can be made by methods such as laser ablation inductively coupled plasma mass spectrometry (LA-ICP-MS). This method allows targeting of different parts of zircon crystals to produce ages of different events that the zircon has been subjected to.

The ages of a zircon grain can be expressed as a ratio between daughter and parent isotopes of lead and uranium. Plotting the two daughter/parent isotopes $^{206}Pb/^{238}U$ and $^{207}Pb/^{235}U$ against each other provides an internal control of the age of the zircon and is called the concordia line on a Wetherill concordia diagram. When the two ages of an analyzed grain match up, the age is said to be concordant, and will fall on the concordia line. Analyzes that do not fall on the concordia line are said to be discordant and can be so due to high or low Pb/U ratios in one or both decay systems.

According to Kirkland et al. (2015), magmatic zircons are usually characterized by a Th/U ratio of >0.5, around 0.7–0.9, but exceptions exist, like kimberlitic zircons that can have low ratios of 0.2–1.0, and zircons in carbonatites of the Kola peninsula showing Th/U ratios up to 9000. Metamorphic zircon usually has ratios <0.5, but exceptions exist here as well, especially for high-grade environments. Several things can affect the Th/U ratio of zircon crystals, including the magma composition and the speed of crystal growth, which can reflect whether the zircon was formed in an early or late stage of the magma crystallization. It is also possible to examine the $U_{(zircon/rock)}$ and $Th_{(zircon/rock)}$ ratios, where the contents of the zircon are compared to the whole rock, to estimate zircon saturation temperature as well as classify rocks by lithology.

Zircon morphology and textures

Due to its ability to survive events that often destroys other minerals, zircon grains preserve the geological history of these events as variations of external morphology, and internal structure and texture of the crystals. Factors that can affect the external shape of zircon grains are the crystallization velocity and variations of magma composition and temperature. The

crystallization velocity is believed to affect the elongation of zircon crystals, with higher velocities producing more elongated crystals, while magma composition and temperature are thought to affect the development of different prismatic or pyramidal forms of the crystal (Corfu et al., 2003).

Technologies such as detection of backscattered electrons (BSE) using a scanning electron microscope allows studying of the internal structures and textures of zircon mineral grains. BSE imaging shows variations of the average atomic number of regions in a grain, with brighter areas having a higher average atomic number. The element responsible for these variations is mainly Hf, with U having a secondary effect. Examples of internal textures include growth zoning, xenocrystic cores, subsolidus modification and growth, hydrothermal alteration, and fracturing. The presence of certain internal textures and structures can give clues to things such as variations in magma composition and temperature, fluid interactions, metamorphic events, recrystallization, and more (Corfu et al., 2003).

Geochemical classification

Classification of rocks can be made from major element data according to several different schemes, with one of the most popular being the total alkalis-silica (TAS) plot for igneous rocks, like the one proposed by Middlemost (1994). Using wt% oxides $Na_2O + K_2O$ plotted against wt% SiO_2, rocks can be classified using nomenclature of common volcanic and plutonic rocks.

Further classification of granitoid rocks can be made from schemes such as the one proposed by Frost et al. (2001). By using a classification scheme in three steps according to the contents of FeOt / (FeOt + MgO) (Fe*), the modified alkali–lime index (MALI) ($Na_2O + K_2O – CaO$), and finally the aluminum saturation index (ASI), granitic rocks can be classified into 16 distinct groups. These groups can be used to interpret origin of the magma and tectonic settings. The Fe* is used to discriminate between A-type and Cordilleran type granitoids and can be used when using chemical data that does not distinguish ferric and ferrous iron. The A-type rocks are also known as anorogenic, alkaline or anhydrous type granitoids, because of their presumed anorogenic tectonic origin. Cordilleran type granitoid refers to the batholiths of western North America, characterized by convergent plate boundary magmatism. The modified alkali-lime index can be used to classify the rocks as calcic, calc-alkalic, alkali-calcic or alkalic. This index reflects the different compositions and abundances of feldspars in the rock. The third and final step is the alumina saturation index and classifies the rocks as peraluminous, metaluminous or

peralkaline. The ASI is expressed in the micas and minor minerals of the rock, and it is also related to the origin of the magma, but also the conditions of melting.

Trace element data can be presented using a so-called spider diagram, by plotting the concentrations of Rare Earth Elements (REE) normalized against a chondritic or mantle composition. The REE all form stable 3^+ ions of similar but steadily decreasing ionic radius with increasing atomic number. These small differences in ionic radius produces slightly different behavior of these elements, which fractionates the elements in relation to each other during certain petrological processes. The fractionation patterns can then be interpreted to derive things such as magma origin or hydrothermal interactions (Rollinson, 1993).

Method

Sample collection

Five rock samples were collected at the study area, labeled 22FF002, 22FF003, 22FF005, 22FF006 and 22FF010, and were submitted for whole-rock chemical analysis. Samples 22FF002 and 22FF005 were used for U–Pb dating and closer study for this thesis. The two other samples, 22FF003 and 22FF006 were more closely studied and used for U–Pb zircon dating by Winblad (2022). Samples 16FF46, 21FF001a and 21FF041 were collected by Professor Erik Sturkell and were submitted for whole-rock chemical analysis for this thesis. Sample 22FF010 was collected at the same outcrop dated by the U–Pb zircon ion-microprobe by Hegardt et al. (2007). Sturkell also provided whole-rock chemical data from five additional and previously analyzed samples, which were labeled 12BILL001-003, 12FF71 and 12FF80. Samples labeled GD-1 2018 and GD-2 2018 were analyzed by Leksell & Wennerholm (2018) and used for this study. The samples labeled 12BILL001-003 did not have any GPS coordinates attached to them. During a visit to the site where they were collected, it was confirmed that the site was the same as where GPS coordinates for samples 12FF001-003 were collected. Therefore, the GPS coordinates for samples 12FF001-003 were used for the 12BILL01-03 samples.

Field work

Magnetic susceptibility data were collected in the field area using a handheld digital Gf instruments SM-20 device, and for each outcrop 20 – 40 values were recorded to get representative values for the whole outcrop. Surface unevenness was corrected for according to the user-manual for the device, multiplying with a correction factor depending on the estimated unevenness varying between 1–10 mm.

Gamma ray spectrometry was performed in the field at across the mapped contact between the suites using a RS-230 BGO Super-SPEC Handheld Gamma-Ray spectrometer in Assay mode using a 180 second sample-time setting. The detector was placed directly on the outcrop surface and three measurements were made at each location, recording the values for K (%), U (ppm) and Th (ppm) in the rock. Additional magnetic susceptibility and gamma ray data from the study area were also provided by Professor Erik Sturkell.

Laboratory work

Mineral separation and sample preparation

The two samples 22FF002 and 22FF005, roughly 3–5 kg each, were crushed into powder using a sledgehammer and ring mill, and then sieved through a 420 µm sieve. Zircons were separated

from the rock powder using a Wilfley shaking table, hand magnet, Frantz magnetic separator and finally hand-picking them onto a piece of double-sided tape using tweezers with the aid of a microscope. Epoxy resin was poured into a mold placed on the tape and the tape was removed when the resin was hardened. The resin mound was then polished using a polishing machine. During inspection of the mound using an optical microscope, it was discovered that the number of zircons stuck in the epoxy was low. A new mound was created, but due to time-constraints hand-picking of zircons was not performed. The heavy mineral powder previously created was poured onto a watch glass and a dry 'gravity-separation' was performed, by tapping the glass and separating heavy minerals from lighter. The heavy mineral separate was then poured over double-sided tape and a new mound was created using the same procedure as the previous one. Maps of the resin mounds were made using a Leica DMLP microscope and an Olympus DP-71 microscope camera and stitching together the images in Adobe Photoshop. Finally, the resin mounds were washed with ethanol and prepared with a carbon-coating using a Bal-Tec CED030 carbon thread evaporator.

SEM

Using a Hitachi S-3400N scanning electron microscope (SEM), the zircons were mapped and photographed in preparation for LA-ICP-MS. Zircons were photographed using the backscattered electron (BSE) detector with an accelerating voltage of 15.0 kV and working distance of 9.0 mm.

LA-ICP-MS

The resin mounds with zircons were mounted in an ESL213 laser ablation system connected to an Agilent 8800QQQ ICP-MS, and the maps of the mounds together with the BSE images were used to navigate and mark spots where to ablate the zircons. On 2022-05-23, a total of 48 spots were analyzed, 24 from sample 22FF002 and 24 from sample 22FF005. Some zircons were analyzed multiple times at different spots. The laser spot size was set to 20 µm, with a frequency of 10 Hz and a fluence of 5.7 J/cm^2. The primary standard sample used for calibration was the 91500 zircon crystal, and the age of the crystal is reported by Wiedenbeck et al. (1995) as 1065 Ma. The concordant age found during this thesis for the crystal was 1063±3 Ma, MSWD = 0.17 (N = 26).

External lab work

Whole-rock chemical analysis was performed by the ALS Scandinavia laboratory in Piteå, Sweden, and was performed on samples 22FF002, 22FF003, 22FF005, 22FF006, 16FF46, 21FF001a, 21FF041, and 22FF010.

Handheld XRF

The powder which was left over from crushing the rock samples was analyzed using a handheld X-ray fluorescence analyzer of model Olympus Delta Premium. The instrument was set to Soil mode, which records a total of 25 elements. The three separate beams in soil mode were set for 30 seconds each. Samples were prepared by pouring the powder from each rock into small plastic cups, covered by plastic film on the bottom. The powder was compressed, and the cup was closed with a lid. The samples were then analyzed through the plastic film four times for each sample. These data were then compared to the data from the whole-rock chemical analysis. Many of the elements that the machine tries to quantify, were not detected by the XRF machine, and some were not reported by the whole-rock chemical analysis. These elements were not included in the comparison. The element Fe was excluded from the comparison due to the whole-rock chemical analysis only reporting oxide wt% of Fe_2O_3, and not total elemental Fe. The elements K, Ca, Ti, Cr, Mn, Co, Cu, Zn, Rb, Sr, Zr, Ba and Pb were the ones selected for the comparison, based on previously mentioned limitations, and on what elements can be suitable for differentiation of granitic rocks (Jakob Isaksson, personal communication). For sample 22FF003 Cu was excluded due to less than 1 ppm being reported from the whole-rock analysis, and for sample 22FF005 both Co and Cu were excluded due to the same fact.

Diagrams and data management

GeoChemical Data toolkit (GCDkit) 6.0 using R 3.6.0 was used to create the geochemical classification diagrams, such as TAS-plot and REE chondrite-normalized spider diagram (Janoušek et al., 2006). Samples that had been mapped as mafic in the field were omitted from the geochemical classifications, since the purpose of the classifications were to classify and look for diagnostic trends in the felsic rocks of the Hisingen and Kungsbacka suites.

Igor Pro with iolite 3.7 was used for data-reduction of the raw ICP–MS data. QGIS 3.22 was used to create maps. Adobe Photoshop was used to stitch together images of the resin mounds to create maps. IsoplotR was used to calculate zircon ages and create Wetherill concordia diagrams. In IsoplotR the setting ‘propagate external uncertainties’ was used when calculating concordant and discordia ages. This setting will consider the uncertainties associated with the decay constants and $^{238}U/^{235}U$ ratio. These analytical uncertainties will be shown as a thickness of the concordia line, and these uncertainties will be propagated onto the calculated ages (Vermeesch, 2018). When calculating a regression discordia line through analyzed spots, the setting ‘model-1’ was used. This setting uses the maximum likelihood algorithm for discordia regression after Ludwig (1998).

Results

Zircon morphology

In both samples, intact zircon crystals show euhedral to subhedral crystal habits with elongated to equant shapes. In sample 22FF002 the zircons are commonly of lengths around 150–250 µm, and length-to-width ratios of around 2:1. Both more equant and elongated examples can be found. In sample 22FF005 the zircons are somewhat smaller and more equant, around 100–200 µm with more commonly length-to-width ratios of 1:1 to 2:1. In both samples the zircons show oscillatory growth zoning in BSE images, both in rims and cores. This is interpreted as the zircons being magmatic in origin. Both samples show zircons with BSE contrasting cores compared to the rims, most often with the cores being BSE dark. Both samples also show fractures both in cores and rims, but in sample 22FF005 fractures can commonly be found radiating outward from fractured cores but in sample 22FF002 fractures are more commonly found in BSE dark rims, as fractured overgrowths on euhedral oscillatory zoned cores. Generally, it was easier to find unfractured zircons in sample 22FF005. Zircons with convoluted zoning in cores and oscillatory growth zoning in rims can be found in both samples. Examples of analyzed zircon grains from both samples are shown in Figure 6.

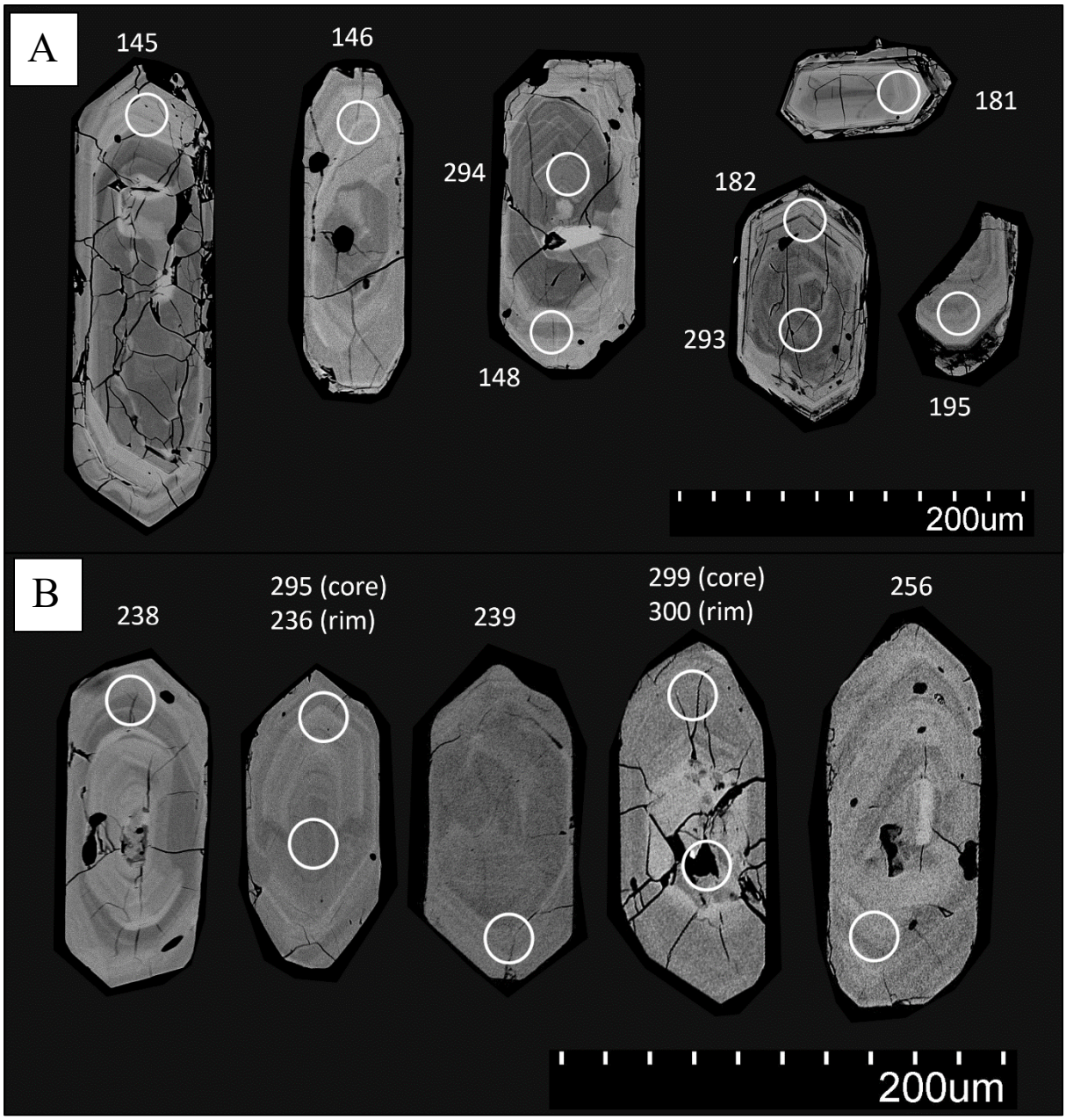

Figure 6. Backscattered electron images (BSE) of examples of analyzed zircons from samples: A) 22FF002 and B) 22FF005. The number shows the spot-numbers that are also presented in Table 4. Circles show analyzed spots. Noticeable features include: generally, BSE dark cores in sample 22FF002, while sample 22FF005 shows less contrast between core/rim, convoluted zoning in cores in zircons marked by spots 145, 148 and 239, euhedral cores showing oscillatory growth zoning with fractured overgrowths in zircons marked by spots 181 and 195, and a fractured core in zircon marked by spot 299.

Zircon geochronology

Sample 22FF002

A total of 22 zircons were analyzed from sample 22FF002, with a total of 24 spots. Fitting a discordia line through all spots using the maximum likelihood algorithm of Ludwig (1998), the upper intercept at the concordia line yields an age of 1562±44 Ma, with a lower intercept at

190±225 Ma, with MSWD = 90. Rejecting spot number 170 due to higher amount of common Pb, and spot number 178 due to low $^{206}Pb/^{238}U$ ratio results in an upper intercept age of 1556±20 Ma, with MSWD = 20 (Fig. 7). Rejecting all >5% discordant spots and fitting a concordia to the remaining 9 spots yields a concordant age of 1556±8 with MSWD = 5.8. The weighted average $^{207}Pb/^{235}U$ age of the same spots yields the same age of 1556±8 with MSWD = 5. When rejecting zircons based on the magmatic Th/U ratio of <0.5, six spots remain, but only three are <7% discordant. Performing a model-1 discordia regression on the six >0.5 Th/U spots yields an upper intercept of 1547±49 Ma, with MSWD = 20. Age data are summarized in Table 2.

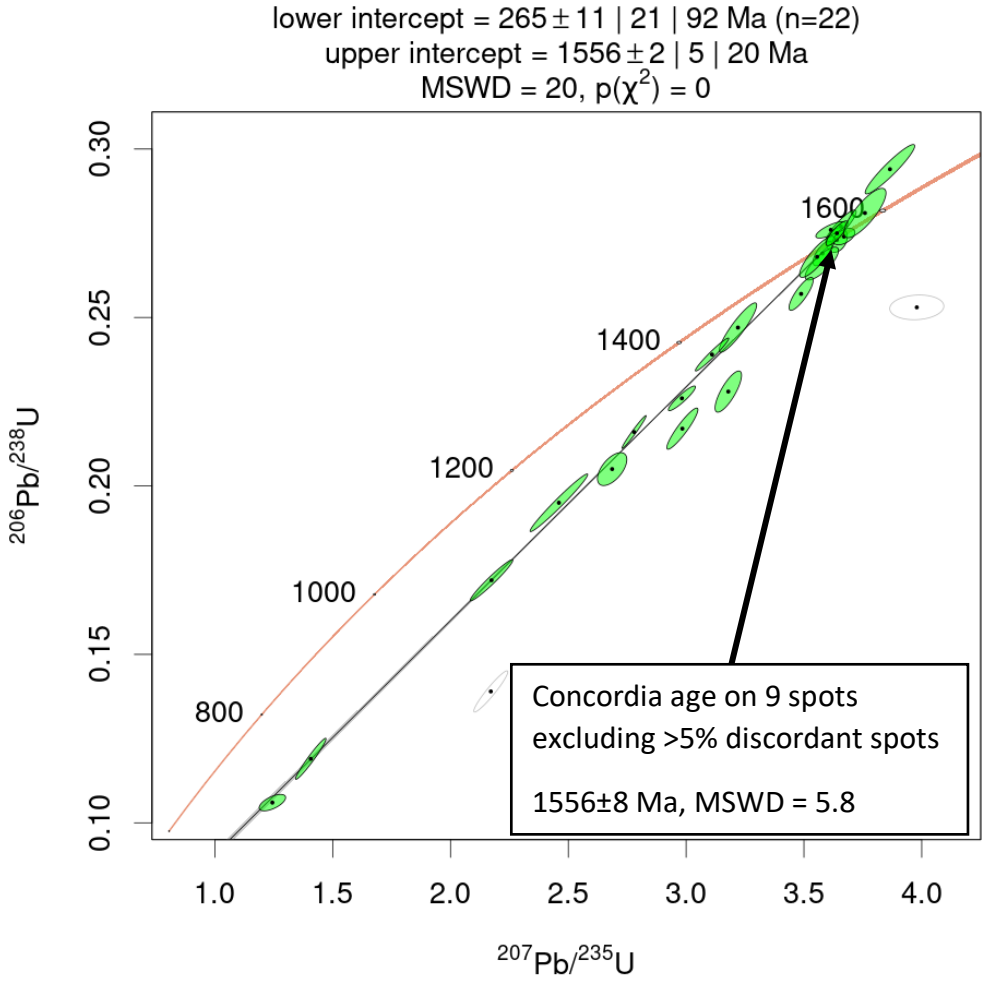

Figure 7. Wetherill concordia diagram of analyzed spots from sample 22FF002. Error ellipses are ±2σ.

Sample 22FF005

24 spots were analyzed in zircons extracted from sample 22FF005, divided amongst 20 zircons. Performing a discordia regression through all the spots yields an upper intercept age of 1551±16 Ma, with MSWD = 10. The zircons in sample 22FF005 are much less discordant than in the

22FF002 sample, with only spot 300 being >5% discordant, which is discordant due to high $^{207}Pb/^{235}U$ ratio. Excluding spot 300 and performing a discordia regression through the remaining 23 spots yields an upper intercept of 1546±12 Ma, with MSWD = 3 (Fig. 8). Using the eight most concordant spots, between -0.86% and 1.6% relative age difference between the $^{206}Pb/^{238}U$ and $^{207}Pb/^{206}Pb$ ages, yields a concordant age of 1557±6 Ma, with MSWD = 2. Calculating the weighted average $^{207}Pb/^{235}U$ age of the <5% discordant spots, and rejecting the spot 300 outlier, (N=22/24) yields an age of 1562±6 Ma, with MSWD 9. When rejecting spots that show Th/U <0.5, 14 spots remain. Rejecting the highly discordant spot 300 and performing a discordia line regression through the remaining spots yields an upper intercept age of 1548±20 Ma, with MSWD = 5.

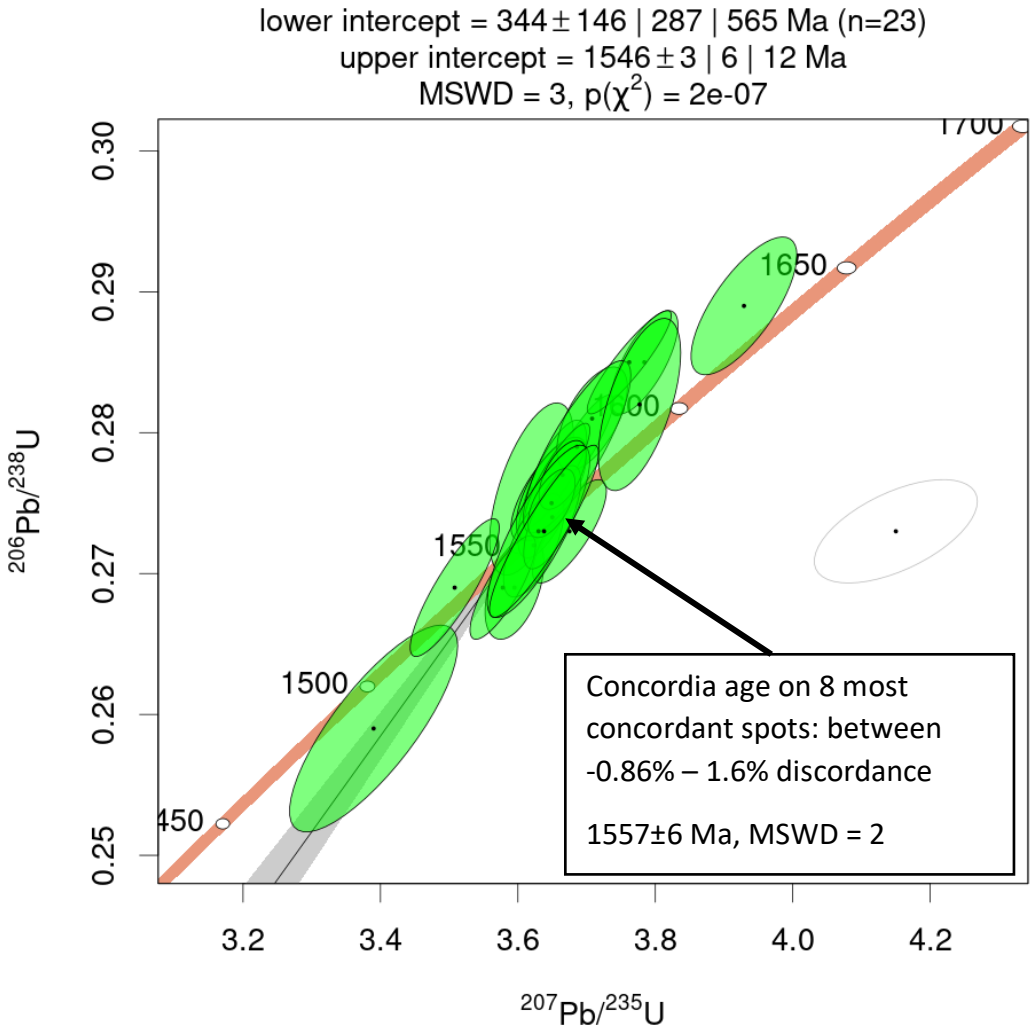

Figure 8. Wetherill concordia diagram of analyzed spots from sample 22FF005. Error ellipses are ±2σ.

Table 2 shows a summary of the ages calculated from the two samples 22FF002 and 22FF005. When calculating the weighted averages of the $^{207}Pb/^{235}U$ ages, outliers were rejected according to a generalized Chauvenet criterion, and a >5% relative age difference between the $^{206}Pb/^{238}U$ and $^{207}Pb/^{206}Pb$ ages were used to reject spots according to discordancy. It can be noted from the table that the 22FF002 sample generally show higher mean squares of weighted deviates (MSWD) values than the 22FF005 sample.

Table 2. Summary of ages from the two samples 22FF002 and 22FF005. Note that the ± age at the 95% confidence interval is calculated with overdispersion, after Vermeesch (2018).

Sample	Age type	Spots used/Spots total	Age (Ma)	±2σ	± at 95% conf. int.	MSWD
22FF002	Upper intercept	24/24	1562	2	44	90
	Upper intercept	22/24	1556	2	20	20
	Upper intercept >0.5 Th/U	6/24	1547	4	49	20
	Weighted average $^{207}Pb/^{235}U$	9/24	1556	2	8	5
	Concordia	9/24	1556	2	8	5.8
22FF005	Upper intercept	24/24	1551	2	16	10
	Upper intercept	23/24	1546	3	12	3
	Upper intercept >0.5 Th/U	13/24	1548	4	20	5
	Weighted average $^{207}Pb/^{235}U$	22/24	1562	1	6	9
	Concordia	8/24	1557	2	6	2

Table 3 shows a summary of the U and Th contents of the analyzed zircons, as well as results from the whole-rock chemical analysis. It shows that sample 22FF002 has higher levels of U when compared to the 22FF005 sample. The zircon/rock ratios are also much higher in the 22FF002 sample. In general, magmatic zircon have >0.5 Th/U, but exceptions exist, see Kirkland et al. (2015) for further information. Possible implications of the Th/U and zircon/rock ratios are considered in the discussion section. Tables 4-1 and 4-2 shows summaries of all the spots analyzed by ICP-MS and shows the isotope ratios and ages in both samples, as well as values for Th/U ratios of the spots and relative discordance. Note the difference of the level of discordancy between the two samples, as well as the more reversely discordant spots in sample 22FF005. Also note the presence of >1600 Ma spots that show relatively low levels of discordancy, like spots 167 and 238.

Table 3. Summary of zircon and whole-rock U and Th chemical data. Note that only a single value of U and Th were reported for each sample from the whole-rock analysis.

		Zircon			Whole rock			Zircon/rock			
		Th	U	Th/U	Th	U	Th/U	Th	U	U/Th	Th/U
Sample		µg/g	µg/g		µg/g	µg/g					
22FF002	mean	253	645	0.448	3.93	2.07	1.90	64.38	311.42	4.84	0.21
	median	250	427	0.438	3.93	2.07	1.90	63.57	206.30	3.25	0.31
22FF005	mean	187	280	0.576	17.65	5.63	3.13	10.58	49.81	4.71	0.21
	median	132	257	0.553	17.65	5.63	3.13	7.48	45.66	6.10	0.16

Table 4-1. ICP-MS zircon isotope and age data from the 22FF002 sample. Note that the errors are reported at the ±2σ level, and not as 95% confidence interval level with overdispersion. Also note the presence of >1600 Ma spots that show relatively low levels of discordancy, like spots 167 and 238.

	Isotope ratios							Ages (Ma)						
Spot	207Pb 235U	±2σ	206Pb 238U	±2σ	207Pb 206Pb	±2σ	Th U	207Pb 235U	±2σ	206Pb 238U	±2σ	207Pb 206Pb	±2σ	Disc. % 1-t68/t76
Sample 22FF002														
145	3.657	0.053	0.277	0.004	0.0961	0.0006	0.367	1562	11	1575	20	1549	12	-1.7%
146	3.640	0.036	0.273	0.003	0.0970	0.0012	0.433	1558	8	1558	15	1565	23	0.4%
147	3.670	0.038	0.274	0.002	0.0973	0.0009	0.354	1565	8	1562	12	1571	18	0.6%
148	3.614	0.052	0.276	0.002	0.0953	0.0009	0.453	1552	12	1569	12	1532	18	-2.4%
149	3.579	0.033	0.269	0.003	0.0964	0.0007	0.402	1545	7	1536	14	1554	14	1.2%
166	3.576	0.058	0.266	0.004	0.0978	0.0010	0.680	1544	13	1520	19	1582	19	3.9%
167	3.865	0.086	0.294	0.006	0.0951	0.0007	0.536	1605	18	1663	31	1528	14	-8.8%
168	3.220	0.065	0.247	0.006	0.0950	0.0010	0.711	1461	16	1423	31	1527	20	6.8%
169	1.244	0.046	0.106	0.002	0.0854	0.0025	0.180	820	20	650	11	1318	54	50.7%
170	3.979	0.094	0.253	0.003	0.1147	0.0034	0.479	1628	19	1455	17	1866	52	22.0%
177	2.174	0.074	0.172	0.005	0.0918	0.0008	0.390	1171	24	1023	28	1463	17	30.1%
178	2.171	0.059	0.139	0.005	0.1140	0.0014	0.480	1171	19	837	28	1863	22	55.1%
179	2.984	0.054	0.217	0.005	0.1001	0.0008	0.618	1403	14	1264	24	1625	15	22.2%
180	2.460	0.100	0.195	0.007	0.0912	0.0009	0.384	1257	30	1147	38	1450	18	20.9%
181	2.686	0.051	0.205	0.004	0.0958	0.0016	0.293	1324	14	1200	19	1543	33	22.2%
182	3.110	0.058	0.239	0.004	0.0944	0.0005	0.492	1435	14	1383	21	1515	9	8.7%
195	1.407	0.053	0.119	0.005	0.0855	0.0008	0.435	891	22	725	26	1326	19	45.3%
196	3.556	0.061	0.268	0.005	0.0964	0.0009	0.515	1539	14	1532	23	1554	17	1.4%
197	3.640	0.038	0.275	0.003	0.0959	0.0006	0.231	1558	8	1567	15	1545	11	-1.4%
198	2.982	0.047	0.226	0.003	0.0959	0.0006	0.948	1402	12	1312	16	1545	12	15.1%
199	3.488	0.042	0.257	0.004	0.0987	0.0009	0.191	1524	10	1476	22	1598	18	7.6%
200	3.179	0.046	0.228	0.005	0.1013	0.0015	0.306	1452	11	1325	28	1645	27	19.5%
293	2.779	0.042	0.216	0.004	0.0939	0.0004	0.443	1350	11	1259	21	1505	9	16.3%
294	3.759	0.073	0.281	0.006	0.0973	0.0012	0.440	1583	15	1597	29	1570	23	-1.7%

Table 5-2. ICP-MS zircon isotope and age data from the 22FF002 sample. Note that the errors are reported at the ±2σ level, and not as 95% confidence interval level with overdispersion. Also note the presence of >1600 Ma spots that show relatively low levels of discordancy, like spots 167 and 238.

	Isotope ratios							Ages (Ma)						
Spot	207Pb 235U	±2σ	206Pb 238U	±2σ	207Pb 206Pb	±2σ	Th U	207Pb 235U	±2σ	206Pb 238U	±2σ	207Pb 206Pb	±2σ	Disc. % 1-t68/t76
Sample 22FF005														
213	3.595	0.035	0.269	0.003	0.0967	0.0010	0.468	1548	8	1536	13	1561	18	1.6%
214	3.620	0.050	0.276	0.005	0.0956	0.0013	0.407	1554	11	1568	23	1539	26	-1.9%
215	3.645	0.045	0.276	0.003	0.0962	0.0008	0.494	1559	10	1568	14	1549	16	-1.2%
216	3.784	0.040	0.285	0.003	0.0963	0.0007	0.454	1589	8	1618	13	1552	14	-4.3%
217	3.690	0.040	0.279	0.003	0.0963	0.0006	0.485	1569	9	1584	16	1553	11	-2.0%
218	3.650	0.041	0.276	0.004	0.0962	0.0009	0.508	1560	9	1571	18	1549	17	-1.4%
236	3.649	0.042	0.276	0.003	0.0961	0.0009	0.699	1560	9	1572	15	1548	17	-1.6%
237	3.708	0.042	0.281	0.003	0.0958	0.0009	0.459	1573	9	1597	15	1543	18	-3.5%
238	3.929	0.063	0.289	0.004	0.0987	0.0011	0.612	1619	13	1636	19	1599	20	-2.3%
239	3.762	0.050	0.285	0.003	0.0957	0.0006	0.652	1584	11	1618	14	1540	11	-5.1%
240	3.657	0.039	0.277	0.003	0.0956	0.0005	0.646	1562	9	1578	13	1539	10	-2.5%
241	3.675	0.044	0.273	0.003	0.0977	0.0007	0.577	1566	10	1557	14	1578	14	1.3%
254	3.623	0.036	0.272	0.003	0.0966	0.0009	0.528	1554	8	1553	15	1558	17	0.3%
255	3.578	0.039	0.269	0.003	0.0966	0.0006	0.582	1544	9	1535	13	1559	12	1.5%
256	3.686	0.064	0.279	0.005	0.0960	0.0010	0.395	1568	14	1587	25	1547	19	-2.6%
257	3.650	0.034	0.274	0.003	0.0967	0.0008	0.703	1560	8	1563	16	1560	15	-0.2%
258	3.665	0.028	0.277	0.002	0.0961	0.0007	0.483	1564	6	1577	12	1547	14	-1.9%
259	3.649	0.028	0.275	0.002	0.0963	0.0007	0.458	1560	6	1566	12	1552	14	-0.9%
295	3.390	0.100	0.259	0.006	0.0955	0.0017	0.473	1502	24	1483	28	1535	34	3.4%
296	3.777	0.049	0.282	0.005	0.0969	0.0013	0.642	1587	11	1602	23	1571	29	-2.0%
298	3.630	0.061	0.273	0.005	0.0965	0.0011	0.625	1555	14	1556	27	1556	21	0.0%
299	3.508	0.053	0.269	0.004	0.0947	0.0008	1.185	1529	12	1534	22	1522	15	-0.8%
300	4.150	0.097	0.273	0.003	0.1100	0.0021	0.615	1663	19	1554	17	1795	35	13.4%
301	3.638	0.065	0.273	0.005	0.0966	0.0007	0.664	1557	14	1557	25	1558	15	0.1%

Magnetic susceptibility and radiometric components

Magnetic susceptibility

The magnetic susceptibility values are between 0.02 and 43.49×10^{-3} SI-units in the study area, with a mean value of 4.82 and a median of 2.46 (Fig. 9). There is a lack of survey points closer to the outcrop dated by Hegardt et al. (2007), but the few points in that area show a generally low magnetic susceptibility. However, there are also outcrops with low values towards the west of the study area, where zircon dating was performed for this thesis. The distribution of all the values in the whole study area show that they concentrate at low susceptibility values.

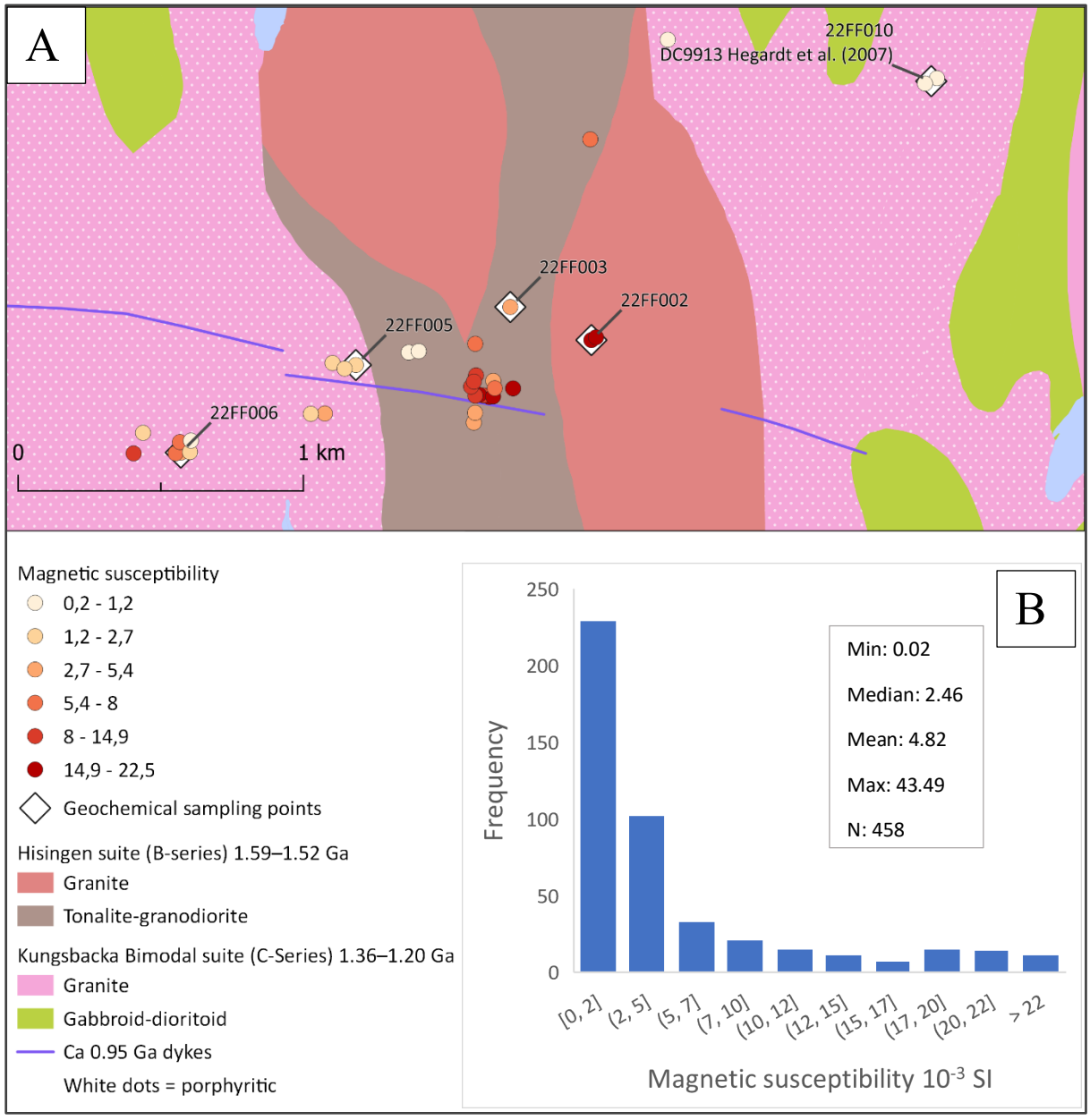

Figure 9. Results of the magnetic susceptibility survey. A) Map of the study area with mean values of outcrops. B) Histogram of all values from field surveys. Background map: SGU bedrock map.

Potassium

The results from the gamma radiation field survey show a normal distribution of the contents of potassium in the study area, with a median value of 3.2% and mean value of 3.4% (Fig. 10). Using the mean values from the outcrops, the max value was found at the outcrop 22FF010, which is the same as the one dated by Hegardt et al. (2007), with a maximum value of 5.4%. Other high values were observed near the outcrop 22FF006, at 5.2%, as well as to the southwest of outcrop 22FF005, at 4.6%. At the 22FF006 outcrop there are high local variations of the potassium content, with values between 2.4–5.2% recorded within 100 m. The lowest values were recorded at outcrop 22FF002, with values of around 1.9–2.0%.

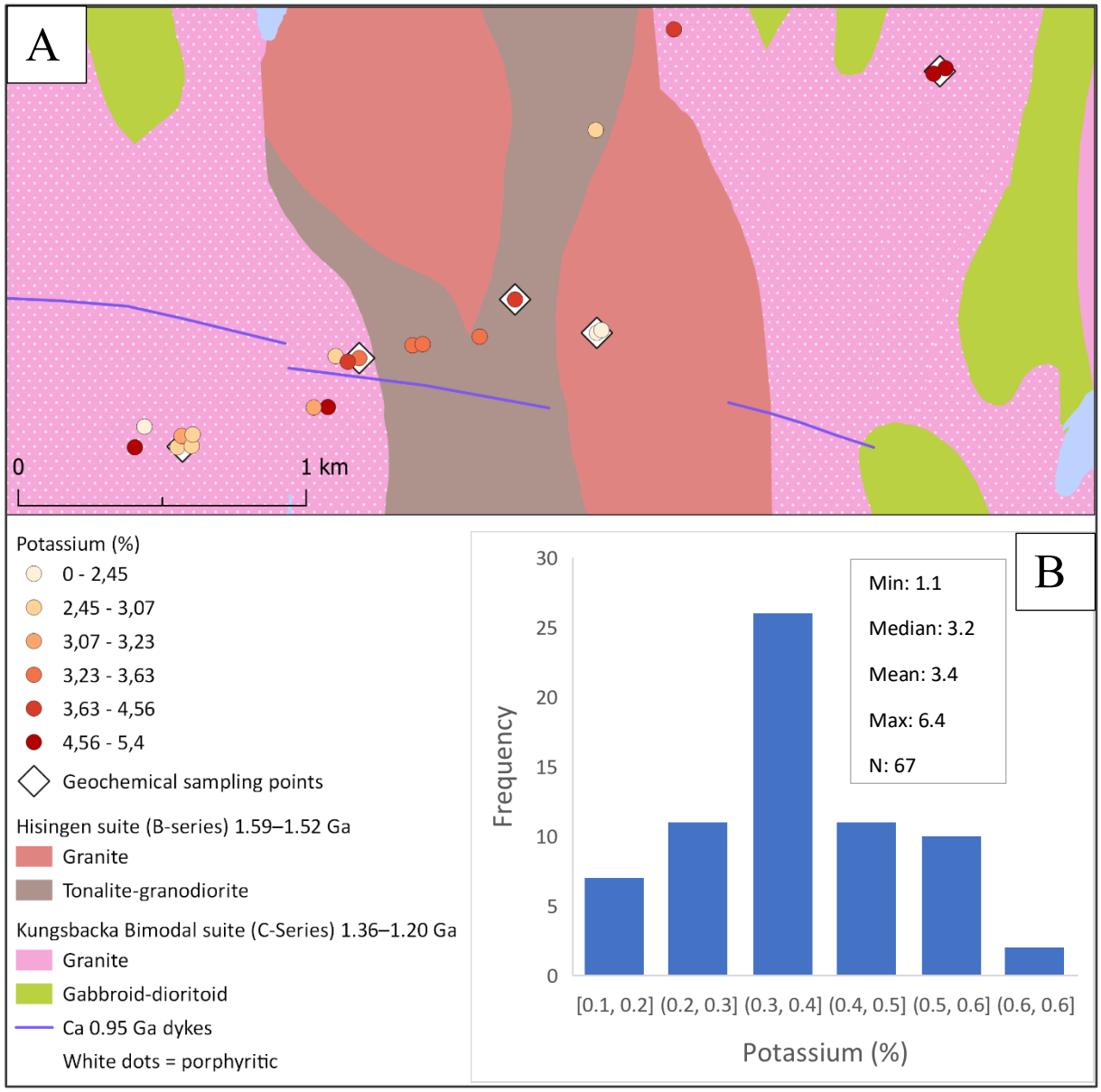

Figure 10. Potassium content results of the gamma radiation survey. A) Map of the study area with mean values of outcrops. B) Histogram of all values from field surveys. Background map: SGU bedrock map.

Uranium

The values for the uranium contents of the outcrops in the study area also seem to be normally distributed, around a median value of 2.9 ppm and a mean value of 3.2 ppm (Fig. 11). The local variation in the area is high, with no obvious spatial patterns. The maximum value was found southwest of the 22FF005 outcrop, at 7.4 ppm, but a value near the mean of 3.2 ppm was also recorded just west of the maximum value. Another example of the high local variation is at the 22FF006 outcrop, where values between 2.2–4.8 ppm U were recorded all within 50 m of each other.

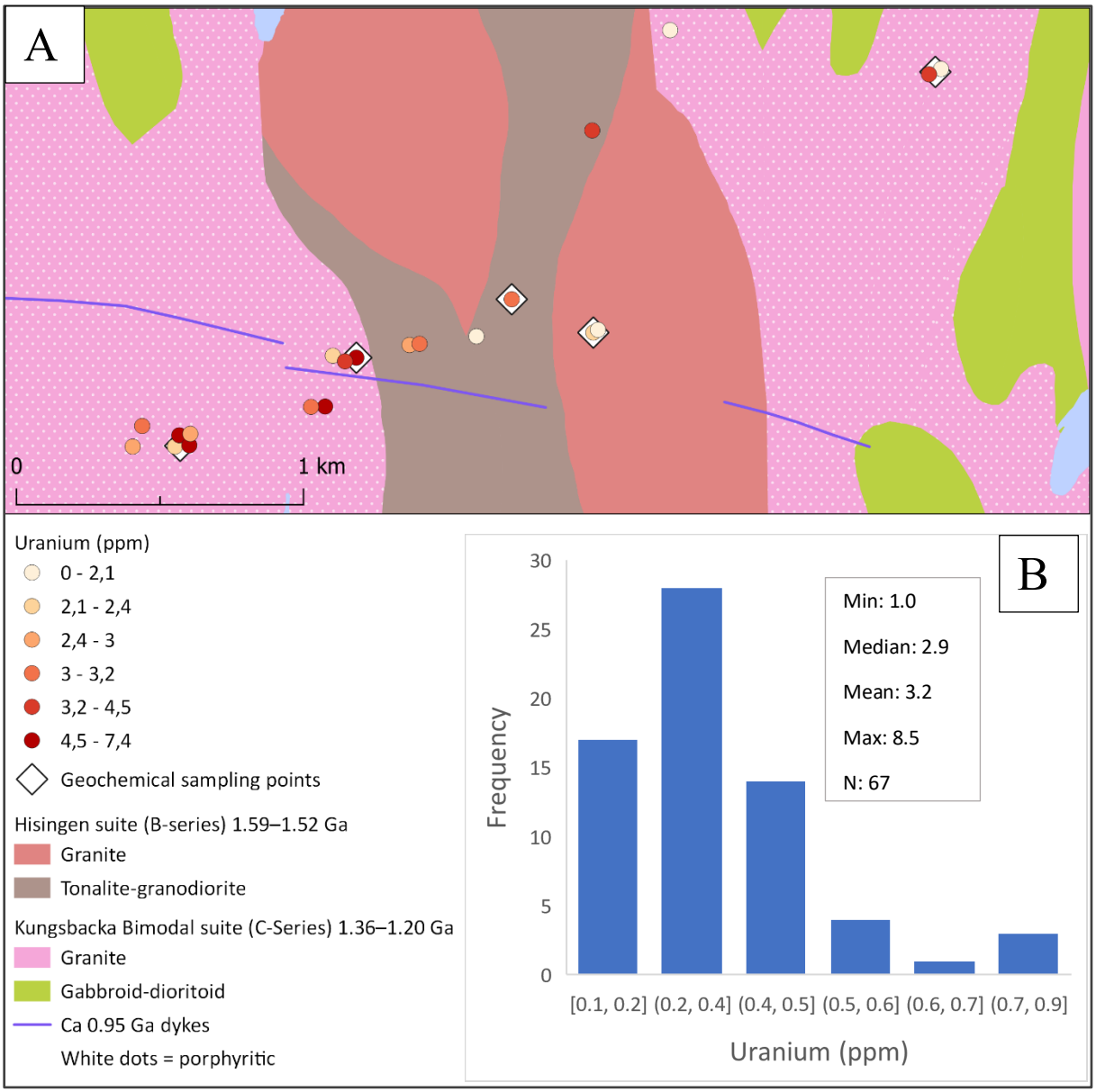

Figure 11. Uranium content results of the gamma radiation survey. A) Map of the study area with mean values of outcrops. B) Histogram of all values from field surveys. Background map: SGU bedrock map.

Thorium

The values of thorium contents are distributed around low concentrations, with a median value of 9.2 ppm and a mean value of 11.2 ppm, but with a maximum value of 38.0 ppm (Fig. 12). The lowest values were recorded at the 22FF002 outcrop, with values between 5.0–6.0 ppm Th. The highest mean outcrop value of 22.5 ppm was recorded to the southwest of outcrop 22FF005. The local variation is also high in thorium, with values being able to vary around 10 ppm within 100 m, near the 22FF005 outcrop. No values typical for the RA-granite were observed (>40 ppm Th), with the highest single recorded value being an outlier at 38 ppm in an aplite vein approximately 1200 m west of the 22FF010 outcrop.

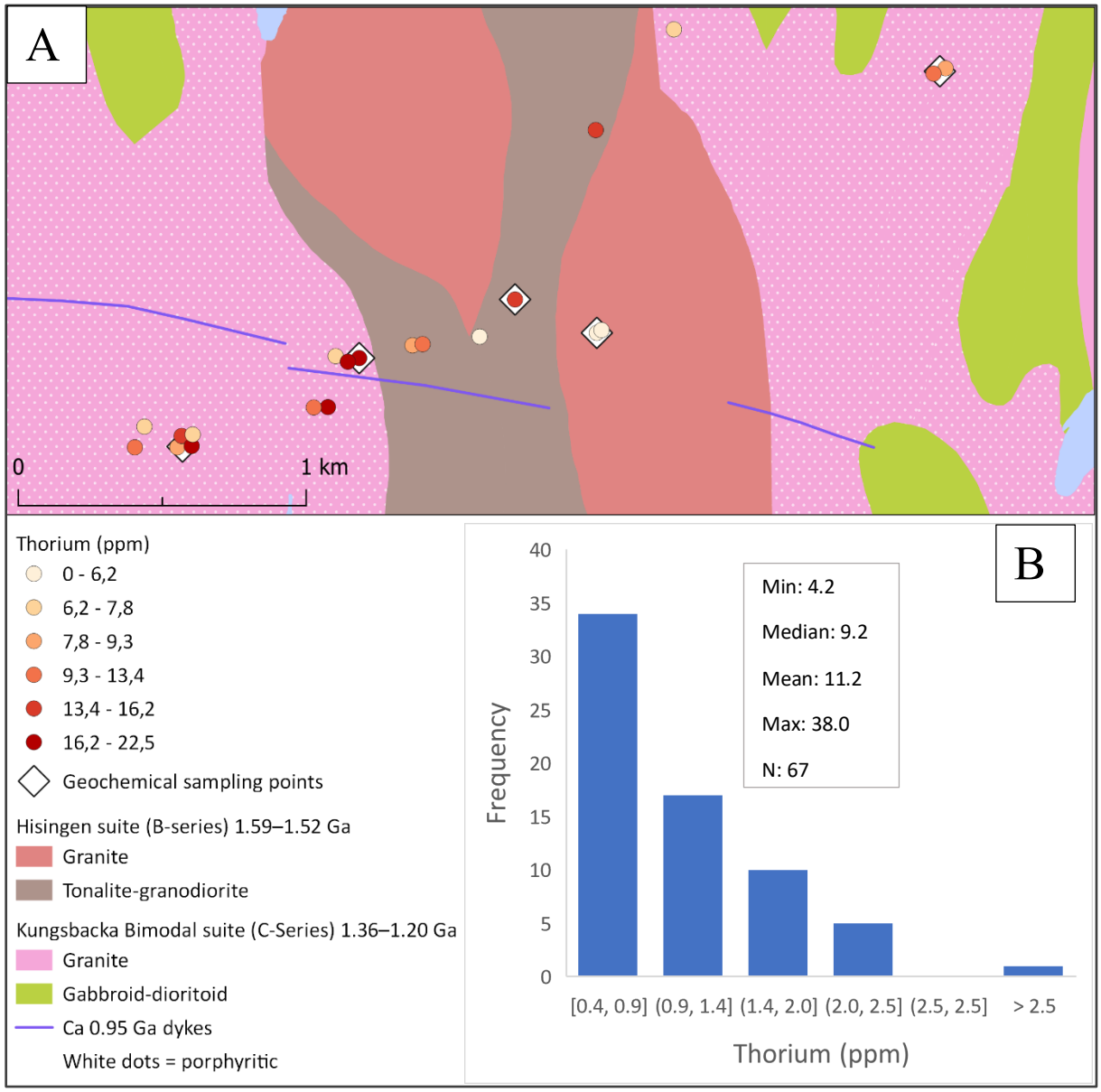

Figure 12. Thorium content results of the gamma radiation survey. A) Map of the study with mean values of outcrops. B) Histogram of all values from field surveys. Background map: SGU bedrock map.

Activity index

The activity index of the outcrops in the study area also shows high local variation (Fig. 13). Most of the values fall below 0.9, with median and mean values of 0.7. The >1.7 value that could be considered diagnostic of the RA granite according to Bergström et al. (2022) could not be found, and values recorded from the 22FF010 Askim granite were also found in the Hisingen suite rocks.

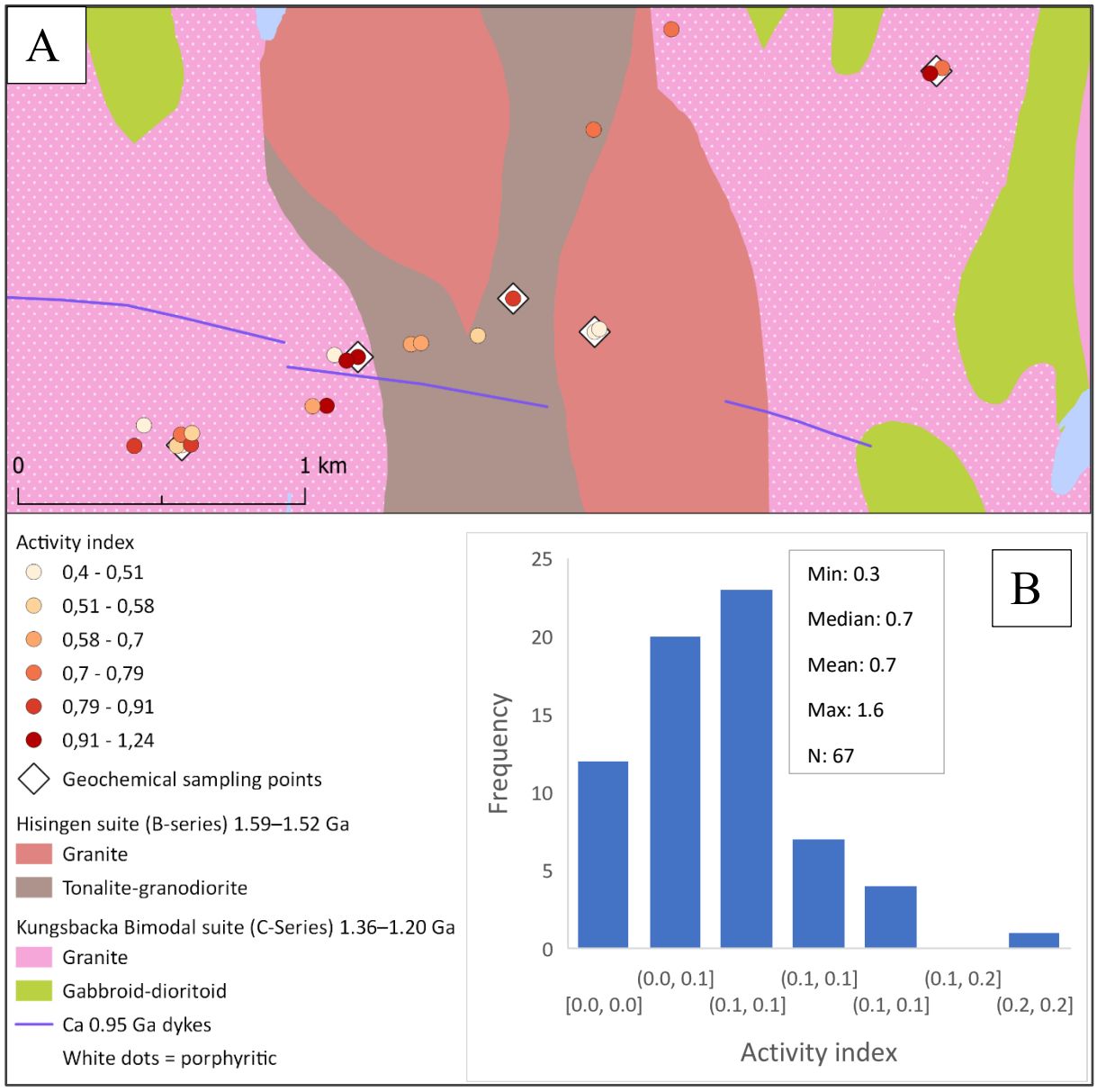

Figure 13. Activity index results of the gamma radiation survey. A) Map of the study area with mean values of outcrops. B) Histogram of all values from field surveys. Background map: SGU bedrock map.

Geochemical classification and whole-rock chemical data

Major element data

The results of the geochemical classification according to the total alkalis-silica (TAS) plot show that rocks group into two compositions: granodioritic and granitic, except for sample 22FF010 which is classified as a quartz monzonite (Fig. 14). Sample 22FF002 was classified as a granodiorite while sample 22FF005 was classified as a granite. The rocks that have been classified as belonging to the Hisingen suite show similar levels of total alkalis but with a wide span of silica. There is a larger range of alkali contents for the rocks classified as the Kungsbacka suite, with the sample 22FF010 at almost 10% total alkalis and the sample 12BILL03 with just over 5% total alkalis.

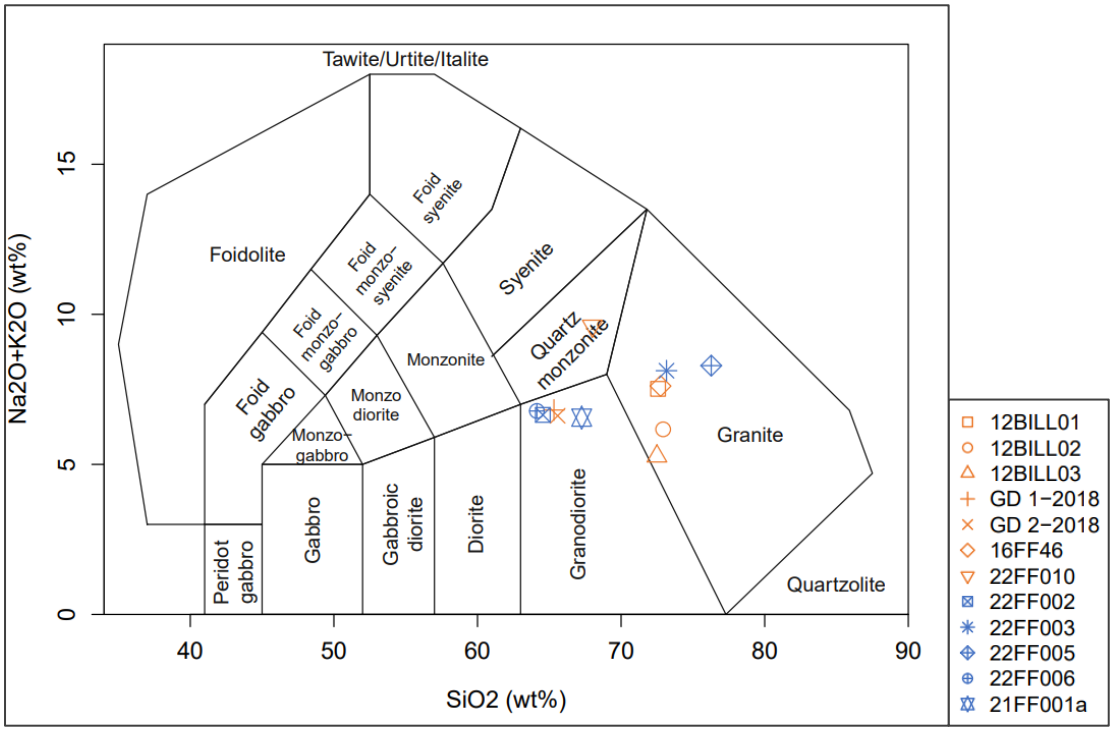

Figure 14. Chemical classification of the whole-rock chemical data of the felsic rocks analyzed. Rocks are grouped by color according to suite. Orange = Kungsbacka suite (C-series), blue = Hisingen suite (B-series). After Middlemost (1994).

The major element data of the rocks in the analysis show that most of the rocks can be classified as felsic according to the silica content, except for 22FF002 that has 63.5wt% SiO2 and could therefore be classified as an intermediate rock (Table 5). It also shows that 22FF010 is an outlier when it comes to potassium content. The Fe_2O_3 contents are high in the rocks that also showing relatively high susceptibility values, 22FF002 and 22FF006.

Table 6. Major element data as wt% oxides of the rocks used for geochemical classification.

SAMPLE	SiO_2 %	Al_2O_3 %	Fe_2O_3 %	CaO %	MgO %	Na_2O %	K_2O %	Cr_2O_3 %	TiO_2 %	MnO %	P_2O_5 %	SrO %	BaO %	Total %
12BILL01	72.9	14.0	2.73	2.1	0.68	3.31	4.24	0.020	0.35	0.04	0.10	0.03	0.1	101.44
12BILL02	73.3	13.9	3.20	2.6	0.84	3.68	2.52	0.020	0.34	0.04	0.12	0.03	0.09	101.68
12BILL03	72.9	14.1	3.25	3.5	0.98	4.03	1.27	0.020	0.40	0.04	0.11	0.04	0.04	101.48
GD 1-2018	65.5	15.9	5.44	4.1	1.70	3.55	3.28	0.020	0.54	0.07	0.20	0.02	0.09	101.76
GD 2-2018	64.5	15.6	5.06	4.1	1.59	3.64	2.87	0.020	0.66	0.07	0.23	0.02	0.08	99.34
16FF46	71.7	13.9	2.39	2.0	0.68	3.41	4.09	0.005	0.30	0.04	0.09	0.01	0.05	99.17
22FF010	68.6	15.2	4.66	1.8	0.31	3.56	6.14	0.002	0.48	0.10	0.07	<0.01	0.14	101.4
22FF002	63.5	16.5	5.28	4.1	1.60	4.58	1.96	0.004	0.63	0.10	0.19	0.03	0.07	99.84
22FF003	72.7	14.0	2.34	1.4	0.51	4.10	3.97	0.004	0.23	0.05	0.07	<0.01	0.05	100.07
22FF005	77.2	13.1	1.23	0.9	0.21	3.67	4.72	0.004	0.14	0.05	0.02	<0.01	0.03	101.59
22FF006	64.7	15.7	5.98	4.6	1.99	3.58	3.26	0.007	0.83	0.10	0.24	0.03	0.11	101.88
21FF001a	67.7	16.2	4.18	3.8	1.41	4.22	2.38	0.005	0.57	0.07	0.16	0.03	0.07	101.4

When plotting the Rare Earth Element (REE) concentrations of the analyzed samples normalized against a chondritic composition, the Hisingen suite rocks are more clustered together and the Kungsbacka suite rocks show a more varied pattern (Fig. 15). Most of the samples show slight or considerable negative Eu anomalies, except for samples 12BILL01, 12BILL02, and 12BILL03, which show no or positive anomalies. The negative Eu anomaly is more prominent in samples 22FF003 and 22FF005. Both suites show very similar concentrations of the lighter REE, except for samples 22FF010 and 12BILL03, which show higher and lower concentrations of the LREE, respectively. For the concentrations of the heavy REE, it seems like the two suites diverge and the Kungsbacka suite is more depleted in the HREE while the Hisingen suite rocks stay at relatively stable concentrations. However, it is only the three samples 12BILL01-03 that get more depleted, while samples 16FF46, GD-1 and GD-2 follow the concentrations of the samples from the Hisingen suite. It also seems like the Hisingen suite rocks diverge somewhat in the HREE, with sample 22FF005 becoming more enriched while sample 22FF003 is more depleted.

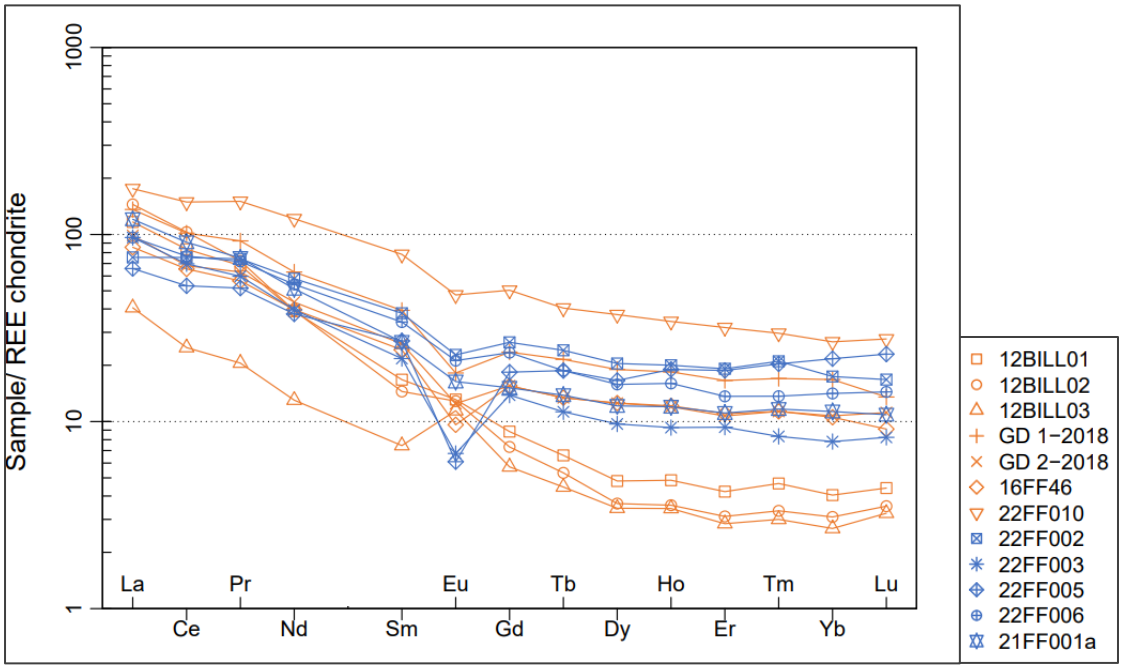

Figure 15. Spider diagram of REE concentrations of the analyzed samples. Normalized against chondritic composition after Nakamura (1974). Rocks are grouped by color according to suite. Orange = Kungsbacka suite (C-series), blue = Hisingen suite (B-series).

The results of the granitic classification following the three step approach by Frost et al. (2001) are shown in Figure 16. The first step is the FeOt / (FeOt + MgO) ratio, which classifies all the rocks as magnesian, except for sample 22FF005 which is border-line magnesian, and sample

22FF010 which is classfied as ferroan. The second step is the modified alkali-lime index ($Na_2O + K_2O - CaO$), and it shows that all of the rocks can be classified as either calc-alkalic or calcic, except for sample 22FF010 which is classified as alkalic. The final step of this approach is the aluminum saturation index (ASI), and the results show that no rocks are classified as peralkaline, and that there is a mix between metaluminous and peraluminous classification across the two rock suites. It can be noted that there seems to be no pattern related to the suite of the rocks, and that the sample 22FF010 seems to be an outlier when it comes to the Fe* and MALI classifications.

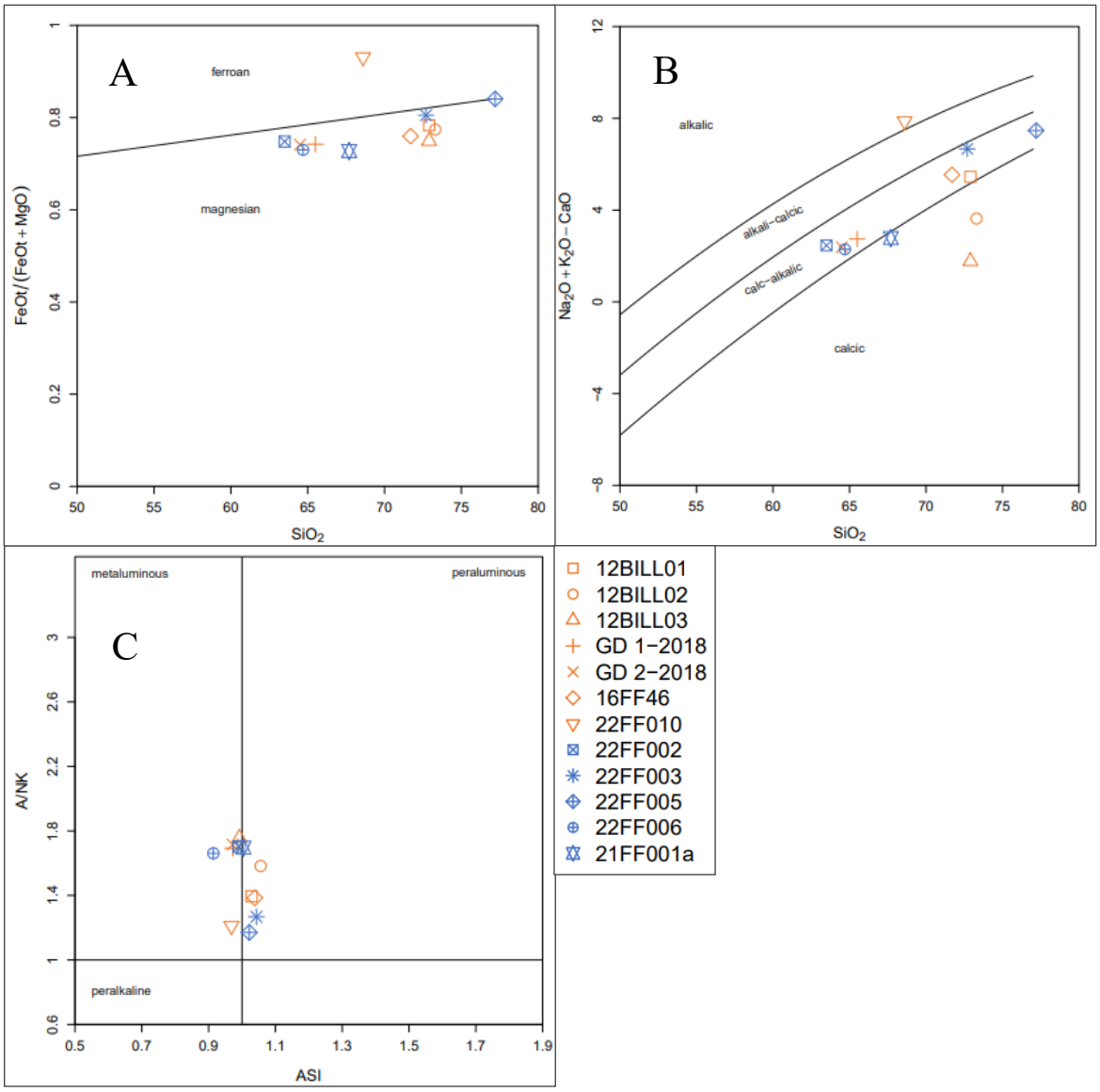

Figure 16. Results of the geochemical classification of granitic rocks after Frost et al. (2001). Classification according to: A) Fe B) Modified alkali-lime index (MALI) and C) Aluminum saturation index (ASI). Rocks are grouped by suite. Orange = Kungsbacka suite, blue = Hisingen suite.*

Handheld X-ray fluorescence

The results from the comparison between the handheld X-ray fluorescence (pXRF) and whole-rock chemical analyses show in general consistent results across all four samples (Fig. 17). Noticeable are the large anomalies for the elements Cr, Co and Cu, and smaller deviations for the elements Zr and Ba. For the other elements the two methods deviate no more than 30% from each other. In general, there is a trend of the pXRF underestimating the contents of the elements compared to the whole-rock analysis. Compared to the other samples, the sample 22FF002 gave the highest value from the pXRF compared to the whole-rock chemical analysis in all elements except Ca, Zn, Sr and Pb.

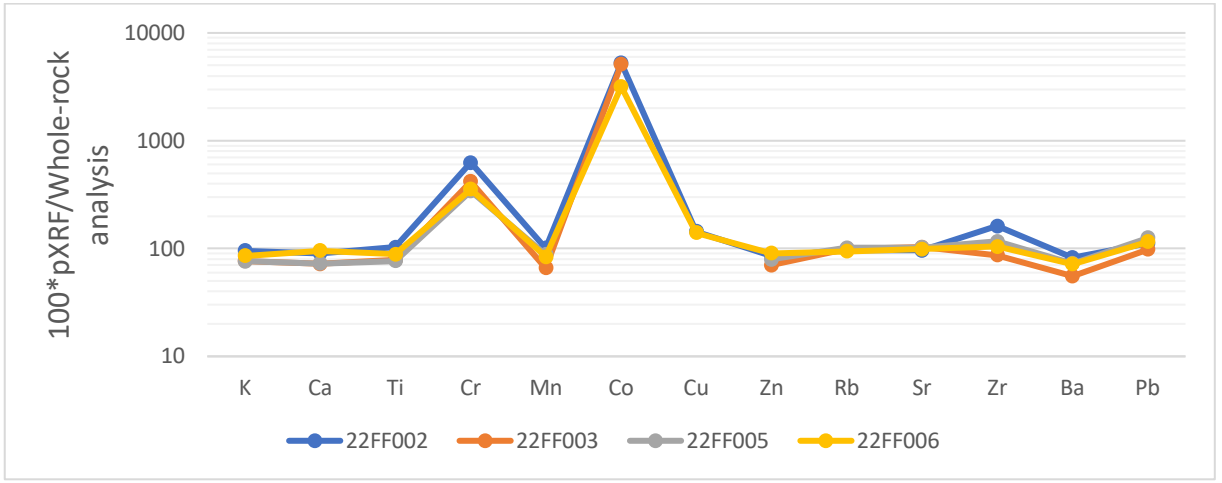

Relative difference (100*XRF/Whole-rock) [%]

Sample	K	Ca	Ti	Cr	Mn	Co	Cu	Zn	Rb	Sr	Zr	Ba	Pb
22FF002	95	90	103	628	101	5266	144	86	97	96	162	82	112
22FF003	77	72	79	419	66	5125		70	100	103	87	55	98
22FF005	76	73	77	341	88			79	101	102	117	73	126
22FF006	86	96	89	356	84	3175	140	90	94	99	104	72	116

Absolute difference (XRF-Whole-rock) [ppm]

Sample	K	Ca	Ti	Cr	Mn	Co	Cu	Zn	Rb	Sr	Zr	Ba	Pb
22FF002	-776	-2820	114	106	7	413	6	-13	-2	-12	159	-112	1
22FF003	-7652	-2767	-290	64	-132	101		-13	0	3	-23	-213	0
22FF005	-9359	-1796	-196	48	-46			-4	3	1	18	-72	4
22FF006	-3852	-1378	-562	102	-126	400	14	-7	-7	-4	14	-269	2

Figure 17. Comparison between handheld X-ray fluorescence and whole-rock chemical analyses

Discussion

Zircon morphology, texture, and geochronology

The morphology of the zircons in the studied samples show many similarities, like the presence of oscillatory growth zoning both in rims and cores. Both samples also show fractured zircon, but the character of the fracturing can differ. The size and length-to-width ratio of zircons are similar, but sample 22FF002 show somewhat larger and elongated grains. Corfu et al. (2003) mentions that needle-shaped acicular zircon is common in rapidly crystallizing systems, like porphyritic sub-volcanic intrusions, high-level granites and gabbros, while more equant grains are more common in deeper intrusions. The grains found in the samples in this thesis are not to be considered needle-shaped however, but the slight observed difference in size and shape could possibly point to different crystallization environments of the two rocks.

The age data from samples 22FF002 and 22FF005 show that the rocks are coeval within 20 Ma when using the biggest span between all the calculated ages. The calculated concordia ages show very similar ages of 1556±8 Ma and 1557±6 Ma, respectively (Table 2). These ages fit right into the span of the Hisingen suite rocks reported at c. 1588–1522 Ma by Bergström et al. (2022) and Bingen et al. (2008), and none of the calculated ages are outside of this span. Both samples can therefore be concluded to belong to the Hisingen suite as there were no ages found around 1300 Ma, which was expected due to where the samples were collected according to the SGU bedrock map. It is also worth noting that the analyzed spots in both samples show no groupings of ages around 1000 Ma, which points to an absence of magmatic activity in this area during the Sveconorwegian orogeny.

When comparing the analyzed spots between the samples, it can be noted that spots from sample 22FF002 shows much higher degrees of discordancy compared to 22FF005. However, sample 22FF005 shows higher levels of reverse discordancy in comparison. The many discordant spots of sample 22FF002 generally follow the discordia line, and it could therefore be an indication of Pb-loss, at the lower intercept of 265±92 Ma. However, the lower intercept is largely controlled by the two spots 169 and 195 as shows a large error. In contrast, the spots of sample 22FF005 show a much tighter grouping around the calculated concordia age. The presence of spots that show ages of >1600 Ma at relatively low levels of discordance in both samples could be an indication of grain inheritance from the older Gothenburg suite.

The zircons from sample 22FF002 contain higher levels of both U and Th compared to sample 22FF005, with averages of 645 µg/g U and 253 µg/g Th in sample 22FF002, compared to 280

µg/g U and 187 µg/g Th in sample 22FF005 (Table 3). This could be why sample 22FF002 shows a higher degree of discordancy compared to the other sample, due to high U and Th contents being able to cause higher degrees of damage from radiation, so called metamictization, by an internal volume increase which causes fracturing, which in turn could cause Pb-loss.

The Th/U ratios of the zircons analyzed in this thesis suggest that the sample 22FF002 could have been subjected to more metamorphic conditions than 22FF005, due to fewer of the zircons from 22FF002 having a Th/U ratio of >0.5 (N=6/24 and N=13/24 respectively), when considering that metamorphic zircon usually has lower Th/U ratio (Kirkland et al., 2015). However, Kirkland et al. also mention that there exist exceptions to this >0.5 Th/U ratio limit. The distribution of the Th/U ratio of our samples show that they all fall within the values normally seen for felsic rocks.

The values of the mean squares of weighted deviates (MSWD) are higher than acceptable for most of the calculated ages. For example, Horstwood (2008), mentions that for a data set with N=5, an acceptable MSWD at the 95% confidence interval would be between 0.2–2.2, and for N=25 it would be 0.6–1.5. All of the calculated ages for sample 22FF002 show a too high MSWD, and all except the calculated concordia are too high for 22FF005, which is borderline. A too high MSWD indicates either that the uncertainties associated with the data points are underestimated, or that there is a real geological dispersion of the data. Also, the errors at the ±2σ level seem too low to be acceptable or realistic. Therefore, the 95% confidence interval with overdispersion is used to present more realistic errors for the ages. As stated by Vermeesch (2018), it is important to mention that overdispersion of geochronological data can point to meaningful geological information, and should not necessarily be seen as negative.

Even when considering the high values of MSWD and possible overdispersion of the data, it can clearly be seen that the ages gather around 1560–1550 Ma in both analyzed samples. Concordia ages found by Winblad (2022) were 1548±2 Ma, with MSWD = 15, for the granitic 22FF003 sample, and 1538±2 Ma, with MSWD = 8.4, for the granodioritic 22FF006 sample. Note that the errors are reported at the ±2σ level. These samples are also within the 1588–1522 Ma range of the Hisingen suite magmatism.

When also considering the ages found by Winblad (2022), which includes the sample 22FF006, well into the mapped extent of the porphyritic Askim granite, it can be concluded that the SGU bedrock map does not show the correct contact between the Kungsbacka bimodal suite and the

Hisingen suite in the western part of the study area, and that all four samples collected and analyzed during both theses belong to the Hisingen suite, and not the Kungsbacka bimodal suite. Considering the age of sample 22FF002 and the date found by Hegardt et al. (2007), there should be a contact of the suites between these two samples. For future research it is therefore suggested to continue mapping in the area, either by continuing west from the location of the 22FF006 sample, or by starting at the 22FF010 (DC9913 by Hegardt et al. (2007)) location and going west, trying to locate the contact to the Hisingen suite from that direction.

Magnetic susceptibility and radiometric components

The mapping of the study area was done with the assumption that the western mapped contact of the Hisingen suite was correct. This resulted in almost all the data points being in the Hisingen suite. Only the 22FF010 outcrop is certain to belong to the Kungsbacka suite. Therefore, the comparison between the suites is very limited for both the magnetic susceptibility and gamma radiation surveys. However, some comments about the results are still discussed below.

There are high local variations of magnetic susceptibility in the rocks in the study area. The outcrops 22FF002 and 22FF006 show slightly higher levels of Fe_2O_3 and are both less felsic than the other rocks in the TAS classification. This could be an indication of higher magnetite contents due to higher iron content in these rocks. The 22FF010 Askim granite show low values of magnetic susceptibility, but these are not diagnostic when compared to the values recorded in the Hisingen suite. The distribution of data points does not show a bimodal distribution that could be suggested to occur if there was a significant difference between suites. It is however suggested for future research that more magnetic susceptibility data are collected, closer to the dated Askim granite, and approaching the Hisingen suite rocks from the west.

The contents of the radiometric components of the rocks in the study area also show a high variability, with both low and high values being recorded in outcrops dated to the Hisingen suite. For the Kungsbacka suite only values from the 22FF010 outcrop are available and show high potassium levels. Low values are seen at the 22FF002 outcrop. These differences are not to be considered diagnostic for differentiation of the suites due to the low amount of sampling points, and due to the variation between the suites seem to be able to be lower than what can be found at the outcrop level. According to Bergström et al. (2022), the Hisingen suite generally seem to have lower potassium contents (Table 1). There is an overlap however, between the more felsic rocks of the Hisingen suite and the more granodioritic rocks of the Kungsbacka

suite. Therefore, no pattern could be found that could be due to significant differences between the suites.

Elevated U and Th levels typical of the Askim or RA granites were not found in the study area and there are outcrops with high variability of these radiometric components. For example, the 22FF010 Askim granite outcrop showed both high and low levels of U. In general, the activity index can be seen as a summary of the contents of radiometric components used to calculate the index. Some outcrops were showing levels above or approaching 1.0 activity index, which according to Bergström et al. (2022) could be considered a diagnostic difference of the suites. Examples of such values recorded is the 0.93 activity index of outcrop 22FF005, with 3.43% K, 4.7 ppm U and 18.7 ppm Th, as well as the value of 1.24 activity index at an outcrop 200 m southwest of outcrop 22FF005, with 4.6% K, 7.4 ppm U and 22.5 ppm Th. These values are not values that would be typical of an RA granite but are elevated compared to the values given for the Hisingen suite by Bergström et al. (2022) as seen in Table 1. The recorded values point to increased contents of radiometric components in the Hisingen suite in certain areas, and could indicate that the values from Bergström et al. (2022) are not diagnostic across the suites. Indeed, as pointed out by the authors, there can be considerable variation of these components, affected by things such as aplite or pegmatite veins. However, generally the Hisingen suite rocks show lower levels of gamma radiation. With this in mind, all three radiometric components, K, U and Th, seem to be normally distributed in the study area, and there is a high variability within outcrops, which indicates no significant difference that could be attributed to a difference in the suites. However, it could still be further examined by continued mapping whether the contents of radiometric components in the Hisingen and Kungsbacka suites can be considered diagnostic.

Geochemical classification

There could be seen no diagnostic grouping of the Hisingen or Kungsbacka suite rocks based on the TAS plot by Middlemost (1994) (Fig. 14). Rocks of both granodioritic and granitic composition occur in both suites. The samples 22FF002 and 22FF006 are less felsic and classified as granodiorites, compared to the 22FF003 and 22FF005 samples, which are classified as granites. This suggests that the extents of the granites and granodiorite-granites in the Hisingen B-series suite in the SGU bedrock map are not correct.

The REE patterns of the rocks from the chondrite normalized spider diagram show some patterns that could indicate differences in the suites (Fig. 15). The samples that were classified as the Kungsbacka suite show similar levels of the LREE as the Hisingen suite, while in the

HREE, three samples assumed to belong the Kungsbacka suite becomes more depleted: samples 12BILL01-03. The 22FF010 Askim granite seems to be an outlier however, in the fact that it shows higher enrichment in the REE, than all other samples. Likewise sample 12BILL03 is an outlier, but more depleted compared to the other samples, except for the positive Eu anomaly. There is an uncertainty due to only one of the samples for the Kungsbacka suite is dated with good results (22FF010), which in this case is an outlier. Samples GD-1 and GD-2 were dated by Leksell and Wennerholm (2018), but it could not be concluded that the granodiorite was within the Kungsbacka bimodal suite. However, the leucogranite samples of their thesis did fall within that range. The other samples are assumed to belong to the Kungsbacka suite because they were collected well within the mapped extent of the suite. The patterns observed show promising results however, and it is suggested that further investigation is made by comparing trace element data of more samples, preferentially with known ages.

Using the classification scheme proposed by Frost et al. (2001), most of the rocks are classified as magnesian calc-alkalic or calcic, except 22FF010 which is classified as a ferroan alkalic metaluminous rock (Fig. 16). Magnesian calc-alkalic rocks were classified by Frost et al. (2001) to commonly occur in the main parts of continental magmatic arc systems, like the central parts of the Cordilleran batholiths in western North America, at convergent plate boundaries. Most rocks in this group are of the I-type granitoids, but there is also considerable overlap with the A-type granitoids in the scheme. Frost et al. mentions that the A-type rocks are much more iron enriched than the I-type, and plot more to the metaluminous field. The difference between metaluminous and peraluminous is not so obvious from the classification, with most samples grouping close to the middle. However, sample 22FF006 is clearly metaluminous, while samples 22FF003 and 22FF005 plot into the peraluminous field.

It is difficult to draw any major conclusions from these element data, due to the lack of data points. Optimally one would collect a high amount of samples and try to identify patterns of the rocks collected, instead of classifying a single outcrop or sample from these diagrams. However, it can be seen from the geochemical classification that the rocks generally follow the magnesian, calc-alkalic trend, except for the outlier 22FF010. The magnesian calc-alkalic rocks are characterized by granite plutons in continental island arc settings, which is also what Åhäll and Connelly (2008) describes as the setting for the major part of the Hisingen suite magmatism at 1588–1522 Ma. Hegardt et al. (2007) describes the Askim granite of the Kungsbacka bimodal suite as having formed in a rift environment. This description matches with what was found for

the sample 22FF010, being geochemically classified as a ferroan, alkalic, metaluminous quartz monzonite. Such a rock is described by Frost et al. (2001) as occurring in within-plate plutons, i.e. anorogenic rocks forming as the result of intraplate rifting. This does not match with how the rest of the presumed Kungsbacka suite rocks were classified, however, and could indicate that they do not belong to that suite, or that the classification used does not accurately classify rocks based on tectonic setting.

Handheld X-ray fluorescence

The results from the comparison between the handheld X-ray fluorescence and whole-rock chemical analysis show that the XRF performs reasonably well when it comes to the elements K, Ca, Ti, Mn, Zn, Rb, Sr, Zr and Pb. It seems to overestimate the contents in sample 22FF002 compared to the other samples, due to it showing the highest relative difference for most of the elements. The reason for this is unknown. For the elements Cr, Co, and Cu the XRF highly overestimates the contents when compared to the whole-rock chemical analysis. The reason for it overestimating Cr could be due to the Cr contents reported from whole-rock analysis being unreliable, due to chromium lined ring mills being used. Co and Cu were also reported in very low amounts from the whole-rock analysis, but the reason for the XRF overestimating these elements is unknown. The elements K, Ca, Rb and Sr can be useful when classifying granitic rocks, and therefore the use of an available handheld XRF could be useful as a first assessment of the contents of these elements, instead of sending them for whole-rock chemical analysis, which can be costly and time consuming. It is important to note that when analyzing the rocks by XRF, rock powder was used, which homogenizes the rock and features such as large phenocrysts are not considered. Due to time constraints a field survey using XRF could not be performed. Examining the viability of handheld XRF field analysis of rocks with large phenocrysts, like the Askim granite or more porphyritic varieties of the Hisingen suite, would be interesting and is one suggestion for a possible future thesis question. Since all four samples analyzed by XRF were found to be of Hisingen suite age, a comparison between the Kungsbacka and Hisingen suite rocks was not made by XRF analysis.

Conclusions

- The two rocks dated by U–Pb zircon LA–ICP–MS were both found to be between 1562–1546 Ma of age, which is coeval with the Hisingen suite continental arc magmatism at 1588–1522 Ma. The 22FF002 granodiorite sample has a concordant age of 1556±8 Ma, MSWD = 5.8, and the 22FF005 granite sample has a concordant age of 1557±6 Ma, MSWD = 2, which can be concluded as them being coeval.
- No diagnostic patterns of magnetic susceptibility or radiometric components were found, but due to low amount of data points it is suggested to continue the mapping of the area and compare values from outcrops with known ages.
- There were no observed patterns of the geochemical classifications between the two suites. The HREE spider diagram pattern showed relative depletion of the three samples 12BILL01-03, compared to samples from the Hisingen suite and Kungsbacka suite. This pattern could be investigated further.
- The handheld X-ray fluorescence analysis of crushed rock shows agreeable results compared to the whole-rock chemical analysis for the elements K, Ca, Ti, Mn, Zn, Rb, Sr, Zr and Pb.

Acknowledgements

Firstly, I would like to thank my supervisor Erik Sturkell, for being supportive, providing guidance and sharing his great knowledge about geology and in particular the regional geology of the Gothenburg area. I also thank my other supervisor Thomas Zack, for providing support and instructions during the LA-ICP-MS, and also for his guidance during the interpretation of the age data. I greatly thank both Mikael Tillberg and Jakob Isaksson for their support and time during the zircon separation, for being available sometimes at such short notice. I would also like to greatly thank my opponent Hanna Tinnerholm for reading my thesis and for her constructive comments both during the seminar and after. I would also like to extend a huge thank you to: my classmate Erika Fondin who provided constructive criticism of my maps and grammar, my brother Oliver Nordqvist who proof-read my thesis, and my partner Josephine Liljekvist Overdick, who tolerated me during the trying times of the writing of my thesis. Lastly, I would like to give a huge thank you to Kristin Winblad for an exciting, at times stressful, but mostly great time during the writing and method work of our theses.

References

Bergström, U., Pile, O., Curtis, P., & Eliasson, T. (2022). *Göteborgsområdets berggrund, jordarter och geologiska utveckling* (SGU-rapport 2021:31). Retrieved from GeoLagret: https://resource.sgu.se/dokument/publikation/sgurapport/sgurapport202131rapport/s2131-rapport.pdf

Bingen, B., Nordgulen, Ø., & Viola, G. (2008). A four-phase model for the Sveconorwegian orogeny, SW Scandinavia. *Norwegian Journal of Geology*, *88*, 43-72.

Corfu, F., Hanchar, J. M., Hoskin, P. W. O., & Kinny, P. (2003). Atlas of Zircon Textures. *Reviews in Mineralogy and Geochemistry*, *53*(1), 469-500. https://doi.org/https://doi.org/10.2113/0530469

Davis, D. W., Krogh, T. E., & Williams, I. S. (2003). Historical Development of Zircon Geochronology. *Reviews in Mineralogy and Geochemistry*, *53*(1), 145-181. https://doi.org/https://doi.org/10.2113/0530145

Frost, B. R., Barnes, C. G., Collins, W. J., Arculus, R. J., Ellis, D. J., & Frost, C. D. (2001). A Geochemical Classification for Granitic Rocks. *Journal of Petrology*, *42*(11), 2033-2048. https://doi.org/10.1093/petrology/42.11.2033

Hegardt, E. A., Cornell, D. H., Hellström, F. A., & Lundqvist, I. (2007). Emplacement ages of the mid-Proterozoic Kungsbacka Bimodal Suite, SW Sweden. *Gff*, *129*(3), 227-234. https://doi.org/10.1080/11035890701293227

Hellström, F. (2009). *Geochronology and petrology of mafic dykes in the Idefjorden Terrane of the Sveconorwegian Province, SW Sweden* (Publication Number A121) University of Gothenburg]. Earth Sciences Centre.

Horstwood, M. S. A. (2008). Data reduction strategies, uncertainty assessment and resolution of LA-(MC-)ICP-MS isotope data. In P. Sylvester (Ed.), *Laser Ablation–ICP–MS in the Earth Sciences: Current practices and outstanding issues* (pp. 283-304).

Janoušek, V., Farrow, C. M., & Erban, V. (2006). Interpretation of Whole-rock Geochemical Data in Igneous Geochemistry: Introducing Geochemical Data Toolkit (GCDkit). *Journal of Petrology*, *47*(6), 1255-1259. https://doi.org/10.1093/petrology/egl013

Kiel, H. M., Cornell, D. H., & Whitehouse, M. J. (2009). Age and emplacement conditions of the Chalmers mafic intrusion deduced from contact melts. *Gff*, *125*(4), 213-220. https://doi.org/10.1080/11035890301254213

Kirkland, C. L., Smithies, R. H., Taylor, R. J. M., Evans, N., & McDonald, B. (2015). Zircon Th/U ratios in magmatic environs. *Lithos*, *212-215*, 397-414. https://doi.org/10.1016/j.lithos.2014.11.021

Leksell, J., & Wennerholm, E. (2018). *Stratigraphic location of Korshamnsberget leucogranite* [Bachelor's Thesis, University of Gothenburg]. Gothenburg. https://studentportal.gu.se/digitalAssets/1737/1737303_b1017.pdf

Lindström, M., Lundqvist, J., Lundqvist, T., Calner, M., & Sivhed, U. (2011). *Sveriges geologi från urtid till nutid* (3. [rev.] ed.). Lund : Studentlitteratur.

Ludwig, K. R. (1998). On the Treatment of Concordant Uranium-Lead Ages. *Geochimica et Cosmochimica Acta*, *62*(4), 665-676. https://doi.org/https://doi.org/10.1016/S0016-7037(98)00059-3

Lundqvist, I., & Kero, L. (2006). *Beskrivning till berggrundskartan 7B Göteborg SV* (K 60). Retrieved from GeoLagret: https://resource.sgu.se/dokument/publikation/k/k60beskrivning/k60-beskrivning.pdf

Middlemost, E. A. K. (1994). Naming materials in the magma/igneous rock system. *Earth-Science Reviews*, *37*, 215-224. https://doi.org/https://doi.org/10.1016/0012-8252(94)90029-9

Parrish, R. R., & Noble, S. R. (2003). Zircon U-Th-Pb Geochronology by Isotope Dilution — Thermal Ionization Mass Spectrometry (ID-TIMS). *Reviews in Mineralogy and Geochemistry*, *53*(1), 183-213. https://doi.org/https://doi.org/10.2113/0530183

Rollinson, H. R. (1993). *Using Geochemical Data: Evaluation, Presentation, Interpretation*. Pearson Education Limited.

Samuelsson, L. (1985). *Beskrivning till berggrundskartan 7B Göteborg NO* (Af 136). Retrieved from GeoLagret:

https://resource.sgu.se/dokument/publikation/af/af136beskrivning/af136-beskrivning.pdf

Vermeesch, P. (2018). IsoplotR: A free and open toolbox for geochronology. *Geoscience Frontiers*, *9*(5), 1479-1493. https://doi.org/10.1016/j.gsf.2018.04.001

Wiedenbeck, M., Allé, P., Corfu, F., Griffin, W. L., Meier, M., Oberli, F., Von Quadt, A., Roddick, J. C., & Spiegel, W. (1995). THREE NATURAL ZIRCON STANDARDS FOR U-TH-PB, LU-HF, TRACE ELEMENT AND REE ANALYSES. *Geostandards Newsletter*, *19*(1), 1-23.

Winblad, K. (2022). *Evaluating methods for classifying granitoids of the west coast of Sweden and U-Pb zircon dating* [Bachelor's Thesis, University of Gothenburg]. Gothenburg.

Åhäll, K.-I., & Connelly, J. N. (2008). Long-term convergence along SW fennoscandia: 330 m.y. of proterozoic crustal growth. *Precambrian Research*, *161*(3-4), 452-474. https://doi.org/10.1016/j.precamres.2007.09.007